ETH zürich

Orbital to spin conversion in magnetic heterostructures

Pietro Gambardella

Department of Materials, ETH Zurich, Switzerland

Shilei Ding
Giacomo Sala
Hanchen Wang
William Legrand
Mingxing Wu
Paul Noël
Federica Nasr
Mingu Kang

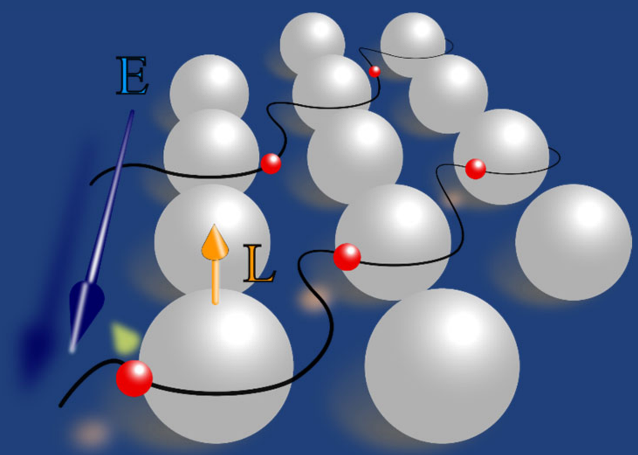

Schweizerischer Nationalfonds

Angular momentum currents

Spin-polarized current

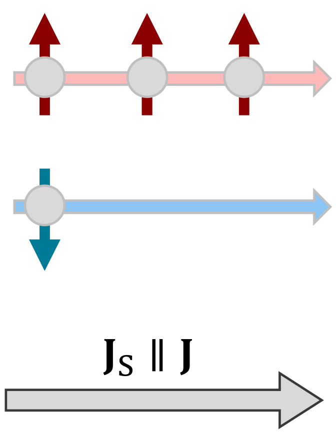

Spin-dependent conductivity in ferromagnets

↓

Charge and spin flow together

(Longitudinal spin flow)

Pure spin current

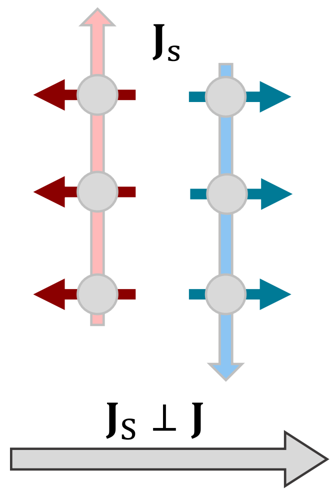

Spin-orbit coupling in nonmagnetic conductors

↓

Decoupled charge and spin flow

(Transverse spin flow)

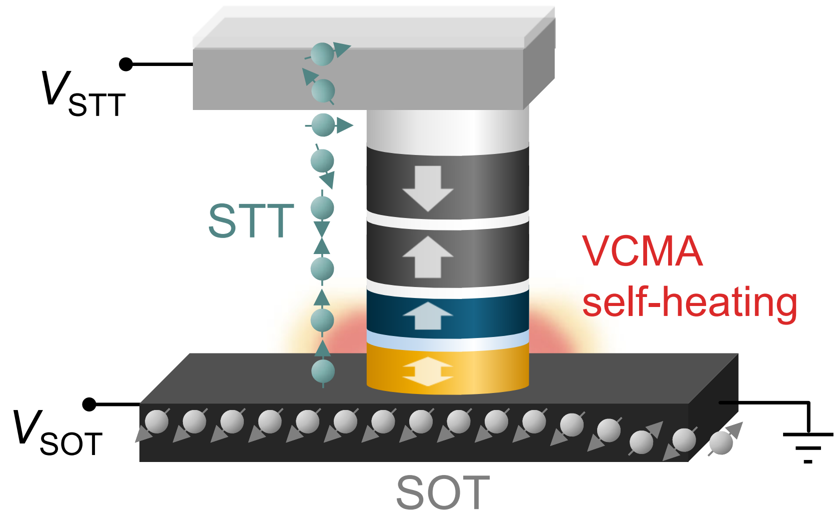

STT	$\propto j_{STT} \propto V_{STT}\,\mathrm{sign}(M_{REF})$
SOT	$\propto j_{SOT} \propto V_{SOT}$
VCMA	$\propto V_{STT}$
Joule heat	$\propto I^2 R$

Krizakova, PG et al.,
Phys. Rev. Appl. **15**, 054055 (2021)

Squeezing switching time distributions by SOT + X

ETH zürich

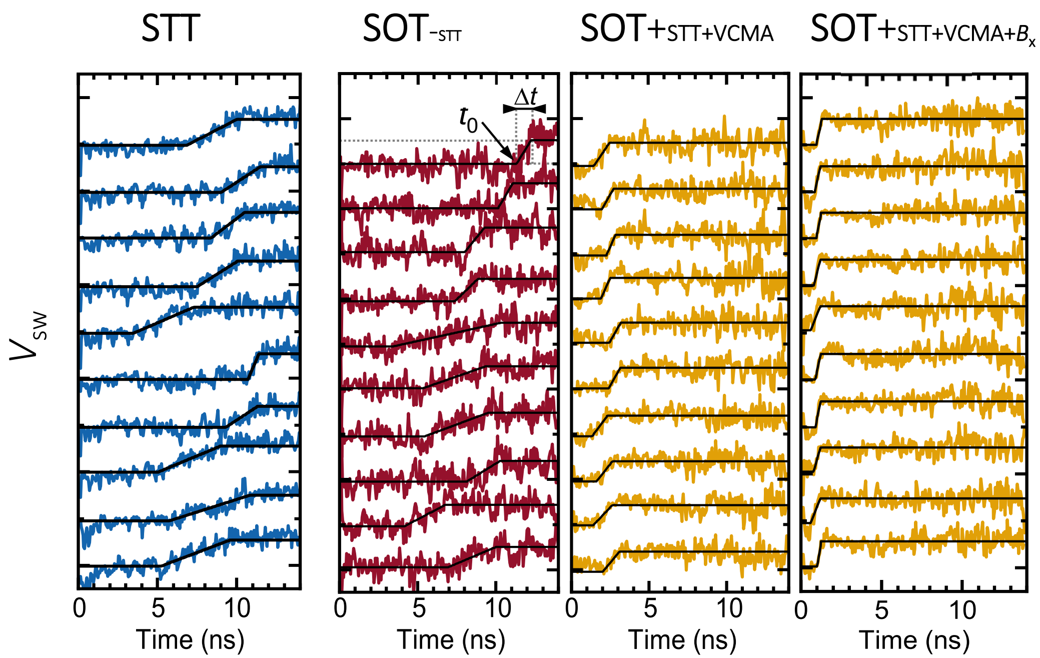

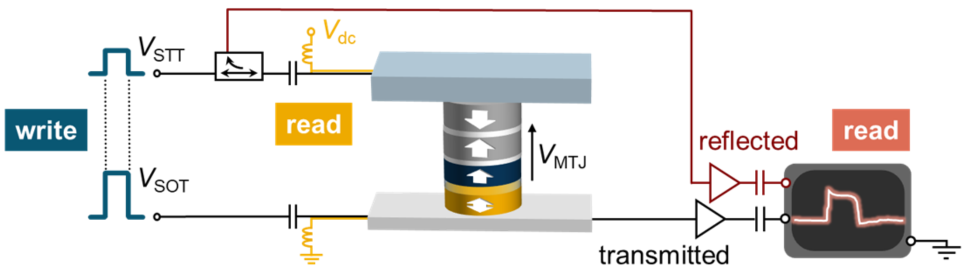

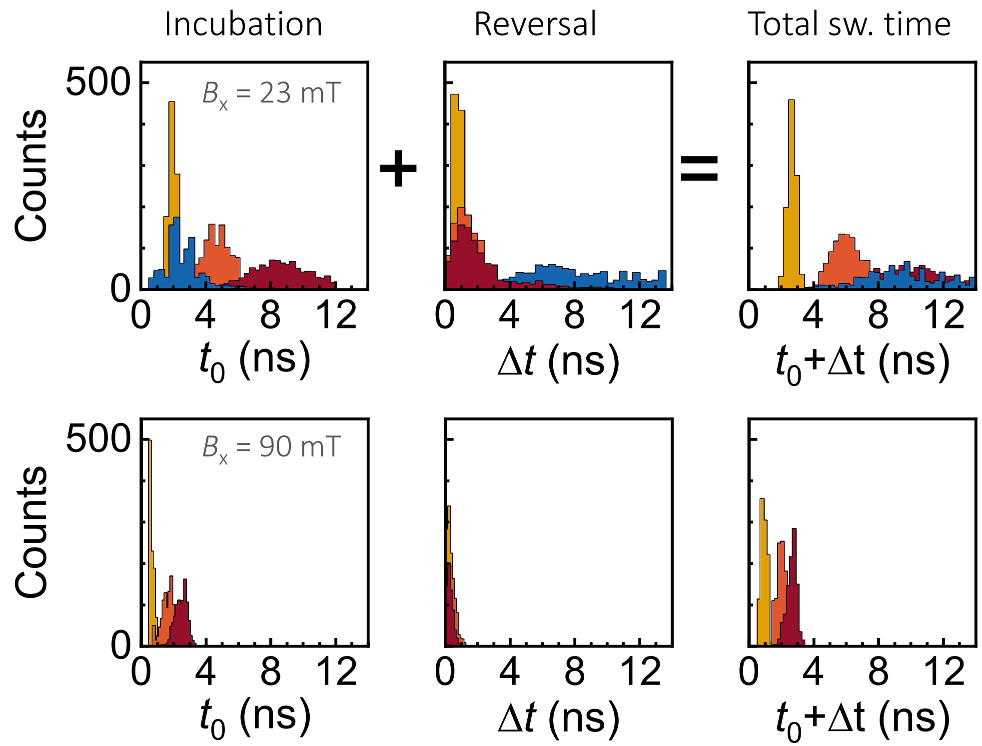

Grimaldi, Krizakova, PG et al., Nat. Nanotech. **15**, 111 (2020)

SOT-induced motion of skyrmions in Pt/TmIG/YIG

ETH zürich

Néel Skyrmion

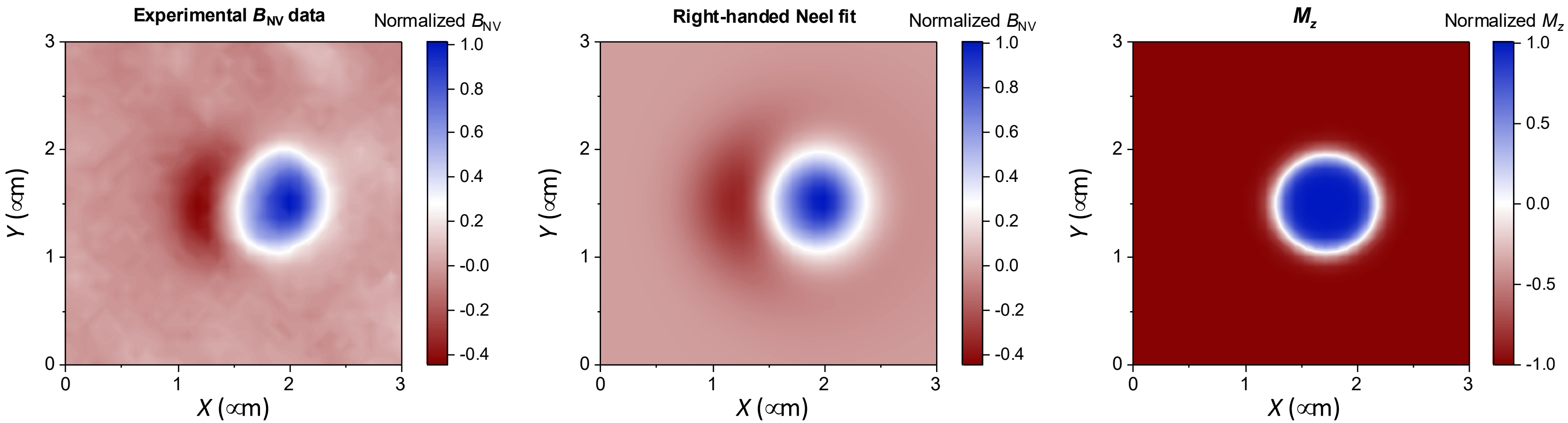

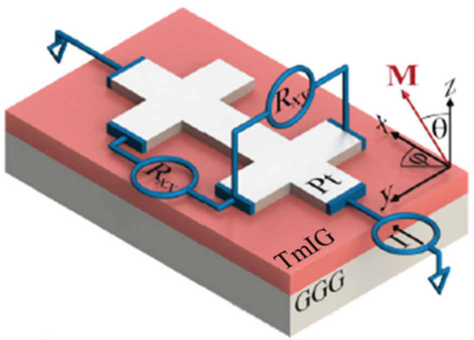

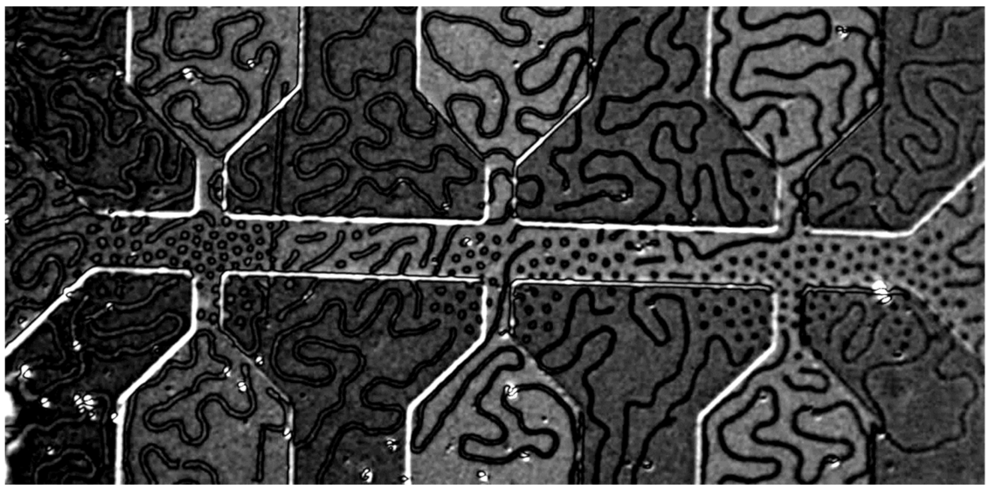

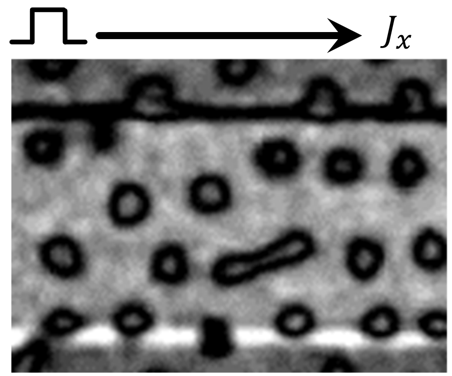

$|J_x|$~ 7x10^{11} A m^{-2}
t_p= 50 ns
H_z = -10 Oe
1 pulse/frame

Vélez, PG et al., Nat. Nanotech. **17**, 834 (2022)

Charge-spin conversion and spin-orbit torques

ETH zürich

Functionalities & Applications

Magnetization switching

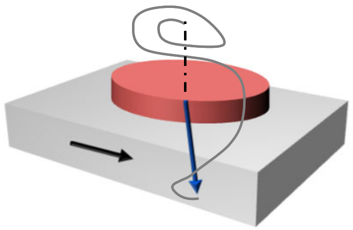

Magnetic memories

High-frequency oscillations

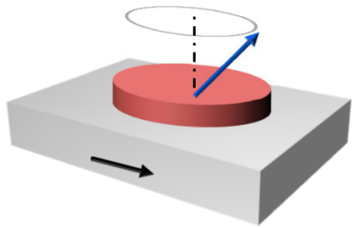

GHz and THz nanooscillators

Domain wall and skyrmion motion

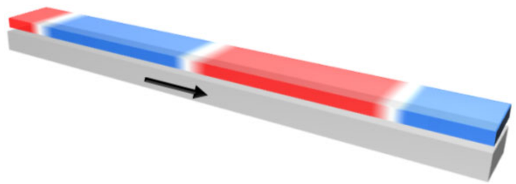

Race-track memories

Spin-wave excitations

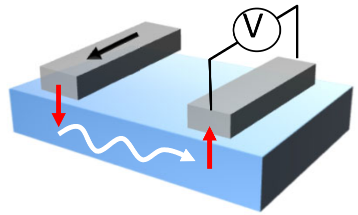

Chargeless interconnect
& spin logic

Materials

Metal and metal-oxide
Heterostructures

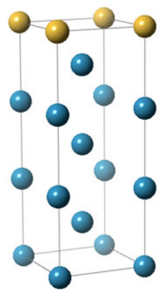

Co, Ni, Fe, GdFeCo...
Ti, V, Cr, … Pt, W, Ta…
WO_x, CuO_x, $SrIrO_3$...
Bi_2Se_3, WTe_2, MoS_2...

Magnetic Insulators
(YIG, TmIG, Bi:YIG…)

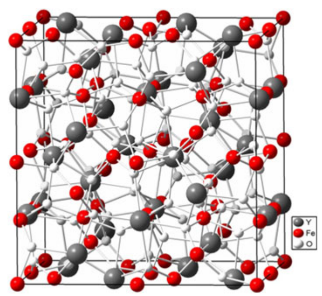

2D Materials

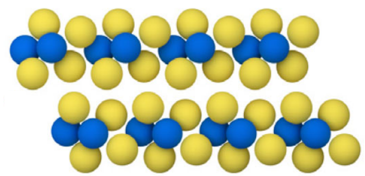

Antiferromagnets
(CuMnAs, Mn_2Au, IrMn, MnPt…)

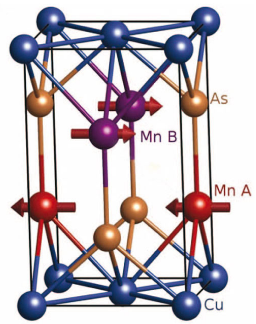

Manchon et al., Rev. Mod. Phys. **91**, 035004 (2019)

Applications of spin-orbit torques

MRAMS

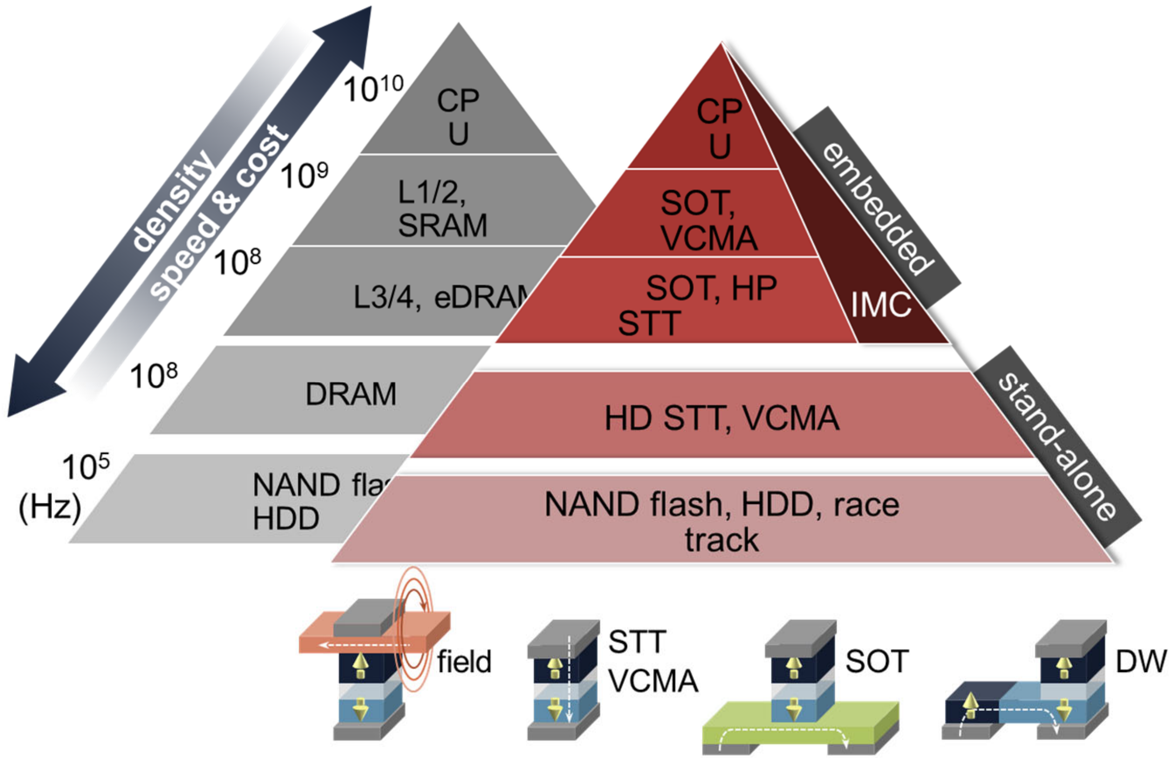

Krizakova, PG et al., *JMMM* **562**, 169692 (2022)

DW logic circuits

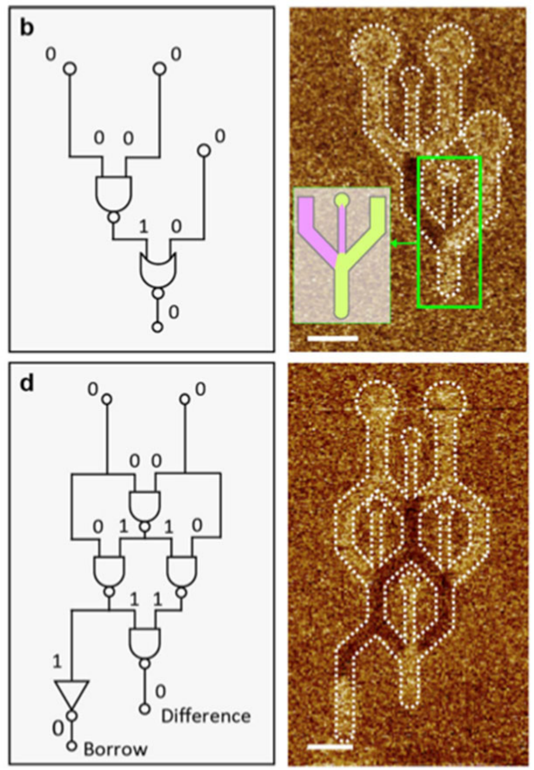

Luo, Hrabec, Heyderman, PG et al., *Nature* **579**, 214 (2020)

ETHzürich

Increasing SOT efficiency and reducing resistivity to improve power consumption

Critical switching current:

$$j_{sw} \propto M_s t_{FM} \frac{H_K}{\xi_{DL}}$$

Lee et. al., *APL* **102**, 112410 (2013)

SOT efficiency:

$$\xi_{DL} = \frac{j_s^{FM}}{j} = \frac{2e}{\hbar} M_s t_{FM} \frac{B_{\mathrm{DL}}}{j}$$

Switching power density:

$$P_{SW} = j_{SW}^2 \rho \propto \frac{\rho}{\xi_{DL}^2}$$

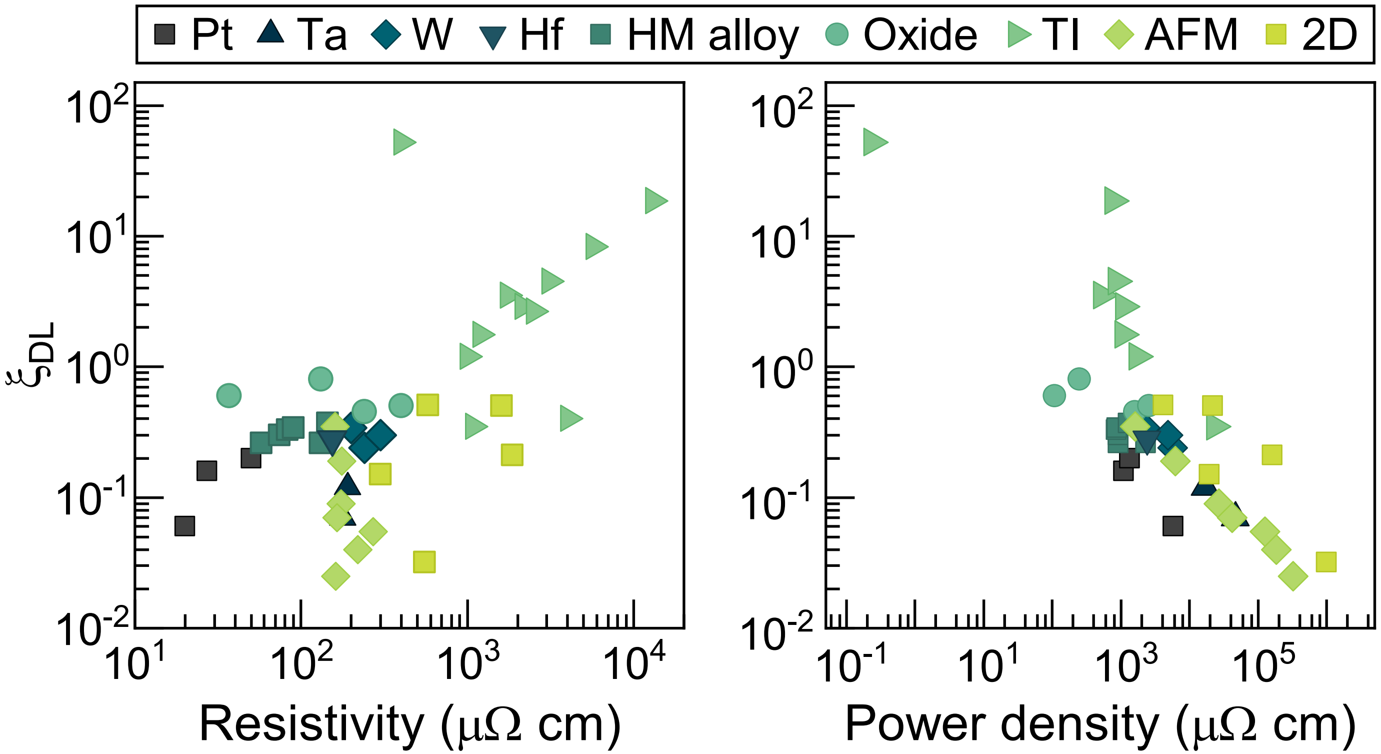

SOT efficiency and resistivity, hence power density, are often correlated → need for large ξ_{DL} low ρ materials

Krizakova, PG et al., J. Magn. Magn. Mater. **562**, 169692 (2022)

Spin-orbitronics

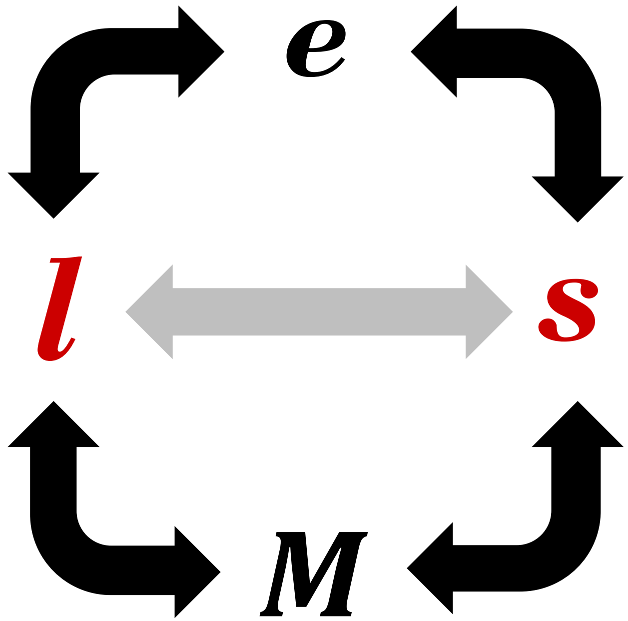

Spin and orbital magnetic moments in transition metals

ETH zürich

Nonmagnetic metals
(Ti, V, Zr, Nb, Mo, Ta, W, Pt, …)

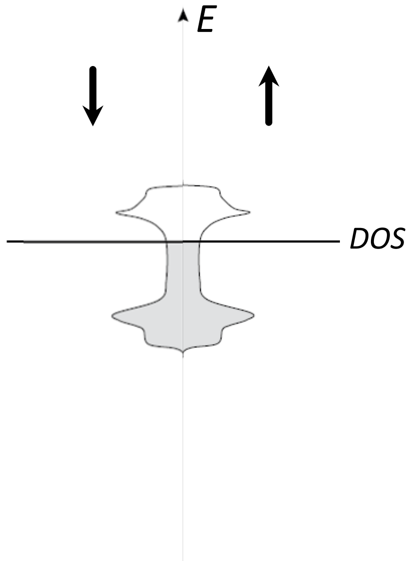

$S = 0$
$L = 0$

Magnetic metals
(Fe, Co, Ni)

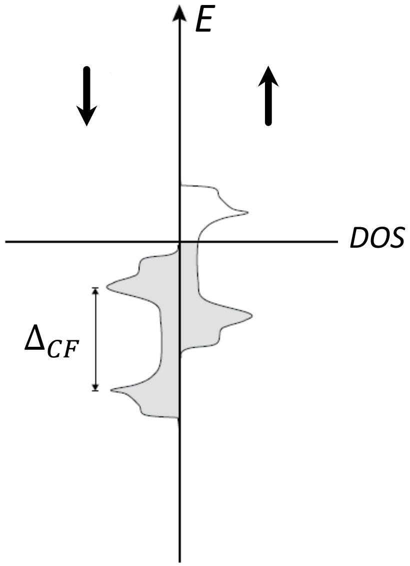

$S \sim 1$

$$L \sim \frac{\lambda_{SO}}{\Delta_{CF}} \approx \frac{0.05\ \mathrm{eV}}{1\ \mathrm{eV}}$$

Element	Free atom	Solid state	m_S (μ_B)	m_L (μ_B)
Fe	$3d^6 4s^2$	$3d^{7.4} 4s^{0.6}$	2.2	0.09
Co	$3d^7 4s^2$	$3d^{8.3} 4s^{0.7}$	1.7	0.15
Ni	$3d^8 4s^2$	$3d^{9.4} 4s^{0.6}$	0.6	0.05

Orbital magnetism

- Orbital magnetic moments in solids

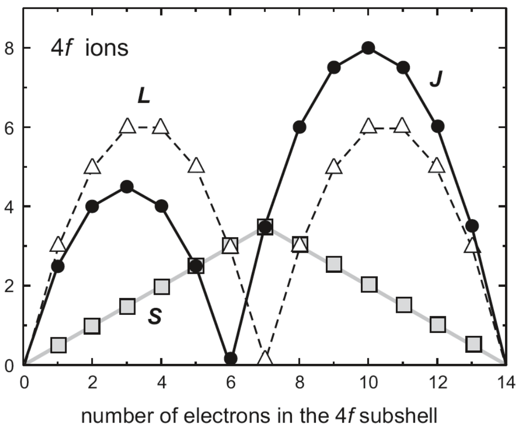

Rare-earths
Atomic-like 4f orbitals

Materials where crystal symmetry preserves orbital degeneracy

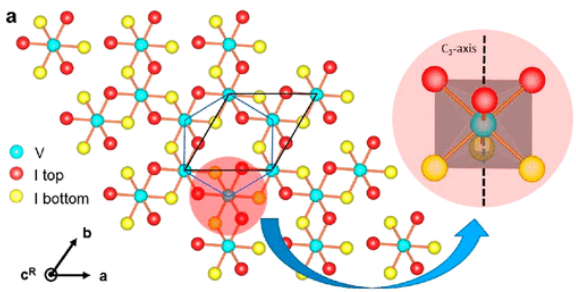

VI_3: $m_L = 0.6\ \mu_B$/V atom
Hovancik et al., *Nano Lett*. **23**, 1175 (2023)

- Magnetocrystalline anisotropy

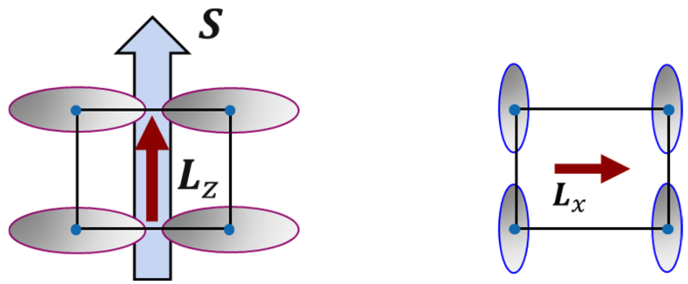

Bruno,
PRB **39**, 865 (1989)

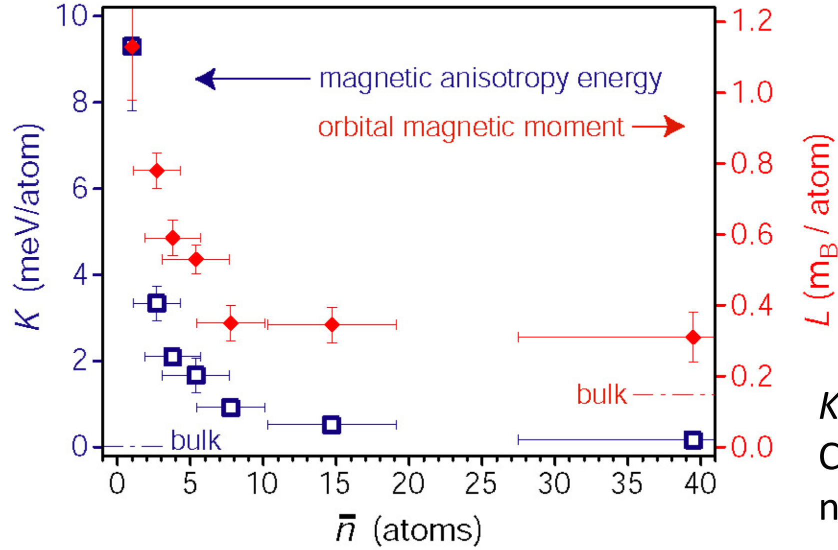

K and *L* in Co_n/Pt(111) nanoparticles

PG et al., *Science* **300**, 1130 (2003)

Angular momentum currents

Spin-polarized current

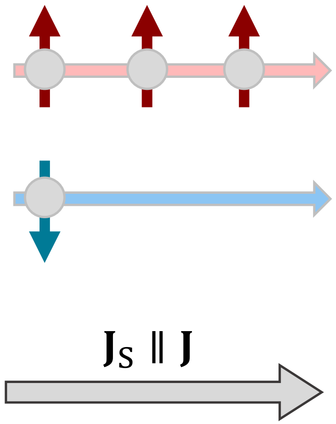

Spin-dependent conductivity in ferromagnets

↓

Charge and spin flow together

(Longitudinal spin flow)

Pure spin current

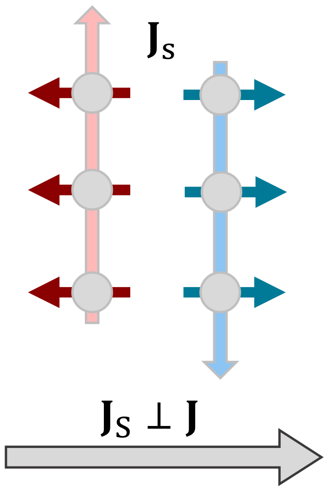

Spin-orbit coupling in nonmagnetic conductors

↓

Decoupled charge and spin flow

(Transverse spin flow)

Pure orbital current

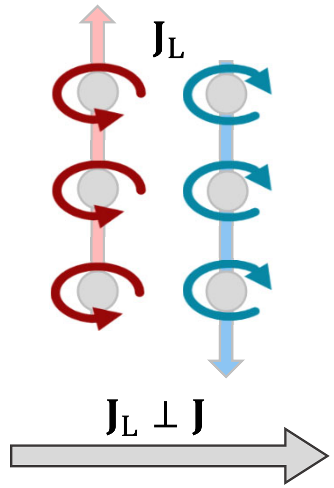

Orbital texture in nonmagnetic conductors

↓

Decoupled charge and orbital flow

(Transverse orbital flow)

Orbital texture of transition metals

ETH zürich

fcc - Ti

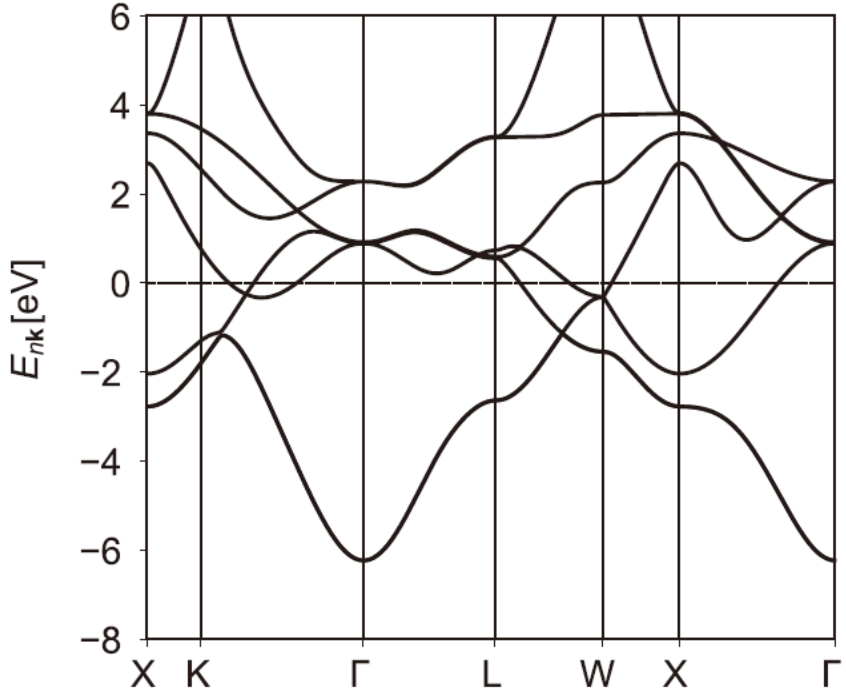

inner Fermi surface of fcc Ti

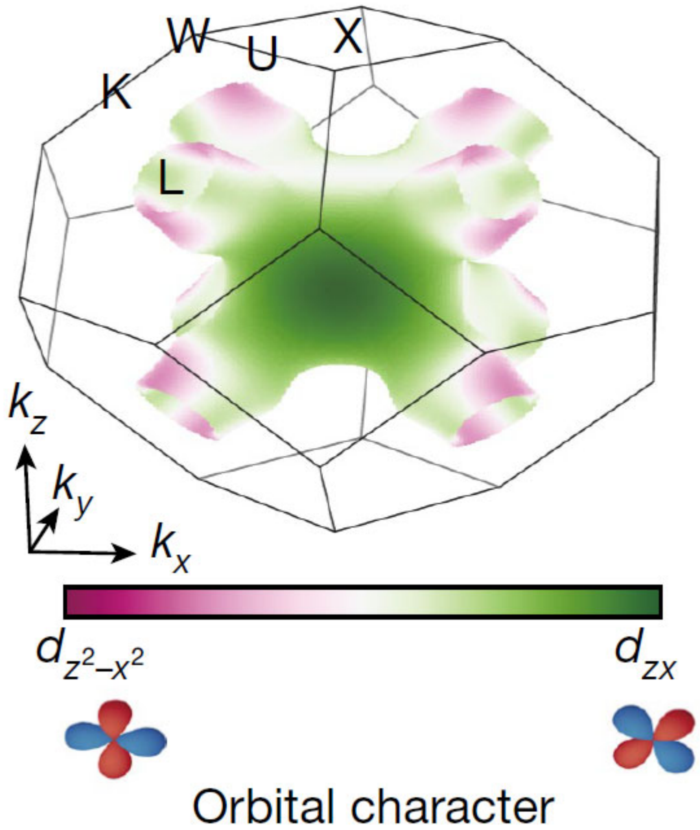

$$|\psi_{n\mathbf{k}}\rangle = C_{d_{xy}\mathbf{k}}\,|\psi_{d_{xy}\mathbf{k}}\rangle + C_{d_{yz}\mathbf{k}}\,|\psi_{d_{yz}\mathbf{k}}\rangle + C_{d_{zx}\mathbf{k}}\,|\psi_{d_{zx}\mathbf{k}}\rangle + \cdots$$

- The coefficients C's are the orbital character of the Bloch state.
- C's are functions of **k** → orbital texture

Go et al., *PRL* **121**, 086602 (2018); Jo et al., *NPJ Spintronics* **2**, 19 (2024);

Choi et al., *Nature* **619**, 52 (2023)

Nonequilibrium orbital dynamics and orbital currents

- Electric fields applied to materials with quenched orbital momenta and space inversion symmetry can generate orbital currents

Bernevig et al., *PRL* **95**, 066601 (2005)
Tanaka et al., *PRB* **77**, 165117 (2008)
Go et al., *PRL* **121**, 086602 (2018); *PRB* **109**, 174435 (2024)
Salemi and Oppeneer, *PR Mater*. **6**, 095001 (2022)
Burgos-Atencia et al., *Adv. Phys. X* **9**, 2371972 (2024)

Pure orbital current

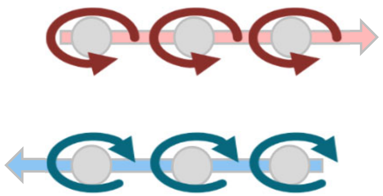

$$\mathbf{J}_{\mathrm{L}} = -\frac{\hbar}{2\mathrm{e}}(\mathbf{J}_{\odot} - \mathbf{J}_{\otimes})$$

$$\mathbf{J}_{\mathrm{c}} = 0, \mathbf{J}_{\mathrm{L}} \neq 0$$

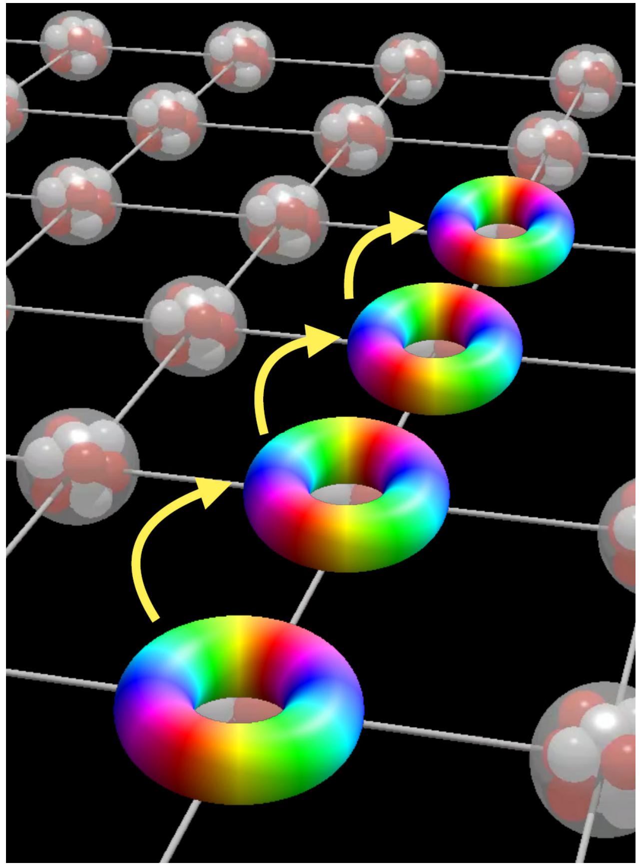

Image courtesy of D. Go, FZ Jülich

Time- and length scales of orbital relaxation in FM and NM materials

ETH zürich

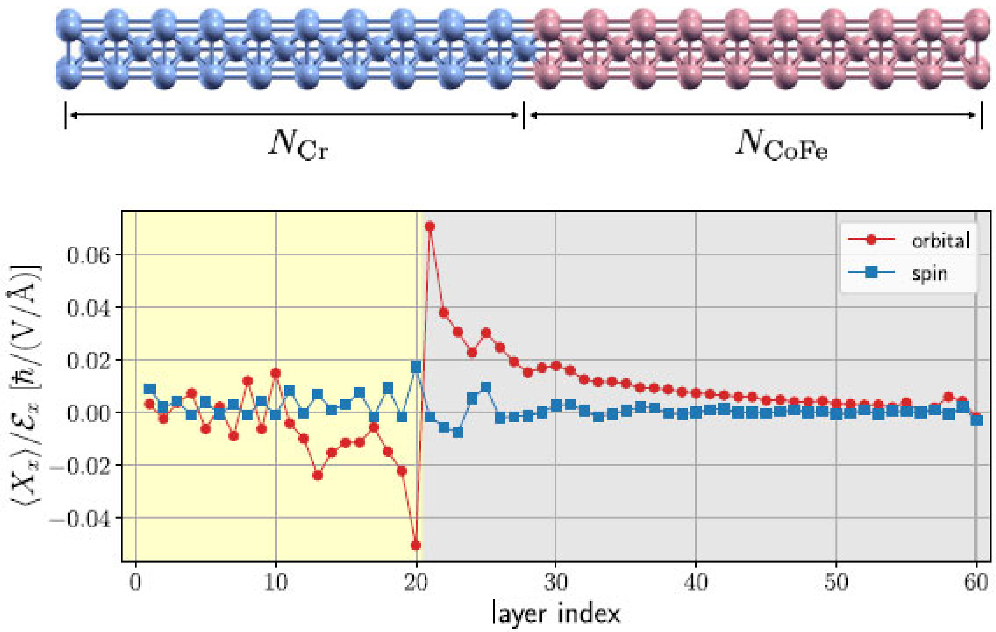

Long-range orbital transport in FM at *k* hot spots

Go et al., *PRL* **130**, 246701 (2023)
Hayashi et al., Comm. Phys. **6**,32 (2023)
Moriya et al., Nano Lett. **24**, 6459 (2024)
Gao et al., Nat. Phys. **20**, 1896 (2024)

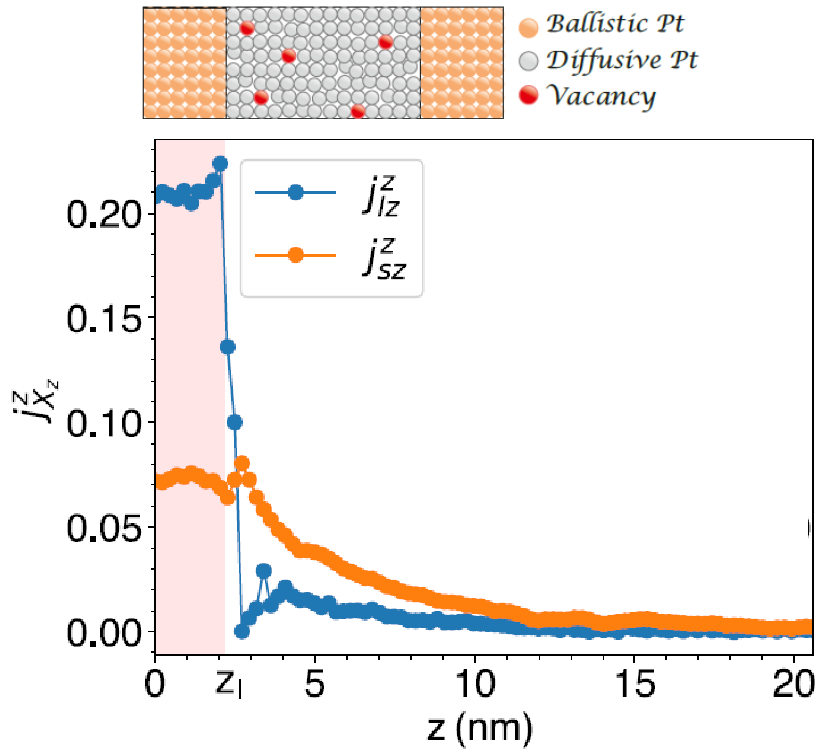

Fast relaxation of orbital current in Pt and partial conversion to spin current

Rang & Kelly, *PRB* **109**, 214427 (2024)
Belaschenko et al., *PRB* **108**, 144433 (2023)
Urazhdin, *PRB* **108**, L180404 (2023)

Alternative models of orbital accumulation

Interface skew scattering:

imbalance between clockwise and counterclockwise electron reflections

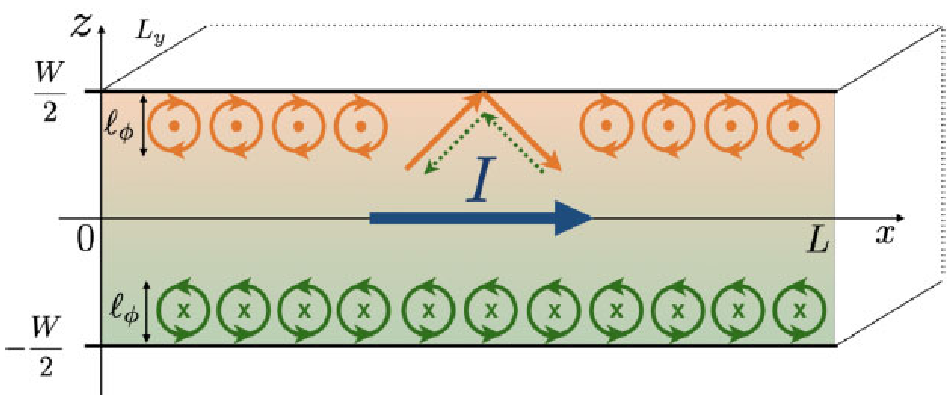

Voss, Adov, and Titov, *PRB* **111**, L121402 (2025)

Interband coherences due to conductivity gradient:

OAM is locally generated by the electron current vorticity through interband quantum processes

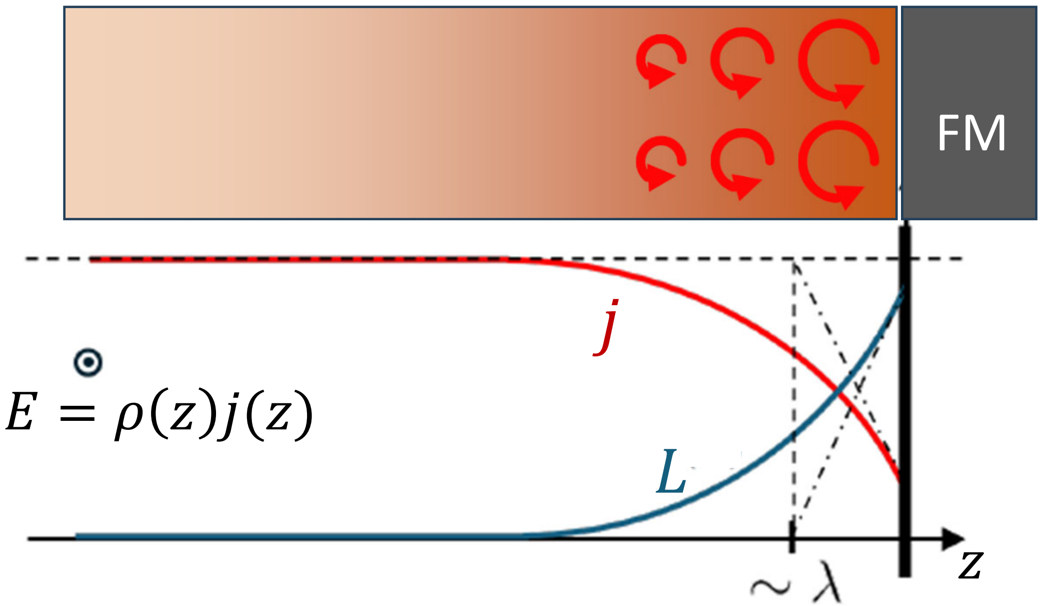

Valet, Jaffres, Cros, Raimondi, arXiv:2507.06771
Valet and Raimondi, *PRB* **111**, L041118 (2025)

Spin and orbital effects resulting in the accumulation of magnetic moments

ETH zürich

SHE

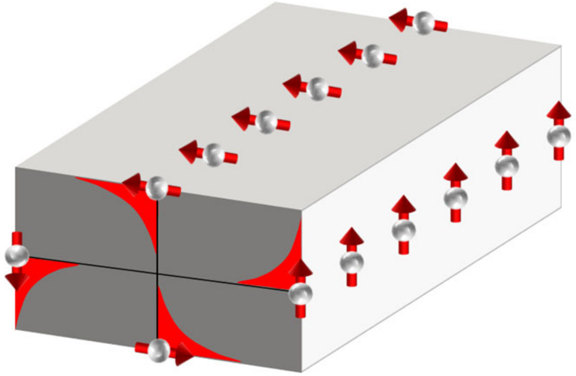

Sinova et al., Rev. Mod. Phys. **87**, 1213 (2015)

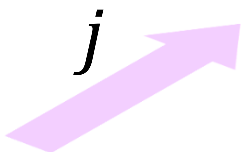

REE

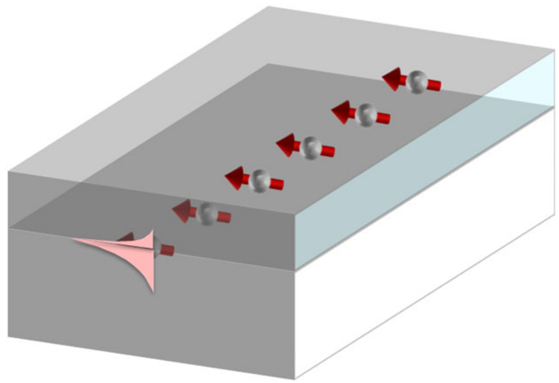

Manchon and Zhang, PRB **78**, 212405 (2008)
PG and Miron, Phil. Trans. R. Soc. A **369**, 3175 (2011)

OHE

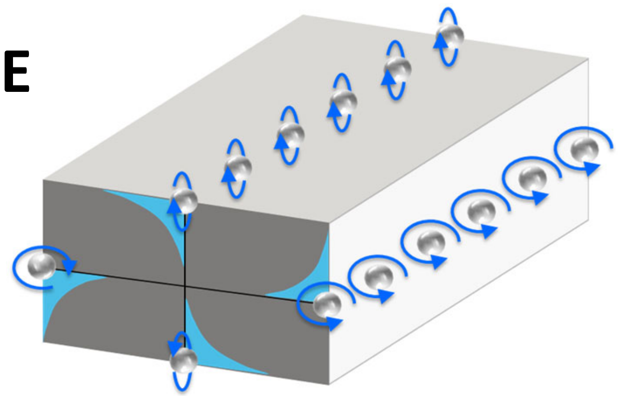

Kontani et al., PRL 1**02**, 016601 (2009)
Go et al., PRL **121**, 086602 (2018)

OREE

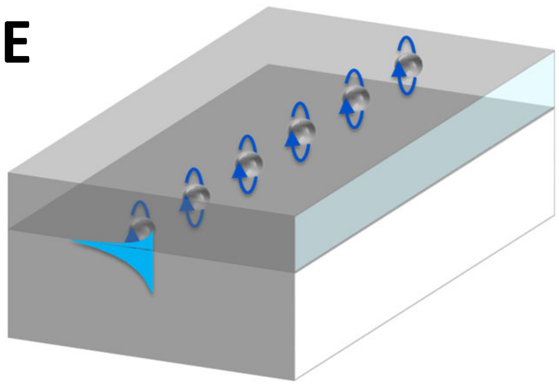

Salemi et al., Nat. Comm. **10**, 5381 (2019)
Johansson, J. Phys. Cond. Matter **36**, 423002 (2024)

Current-induced spin-orbit torques in FM/NM bilayers

ETH zürich

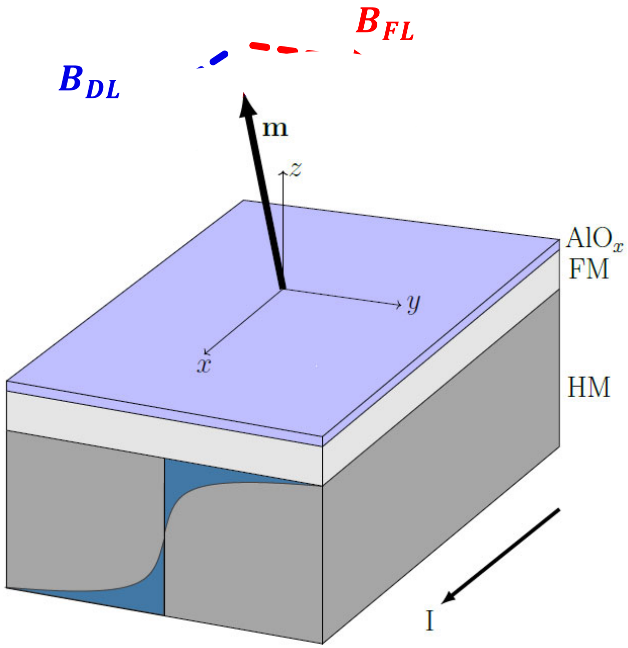

Spin/orbital accumulation
due to “bulk” spin/orbital Hall effect

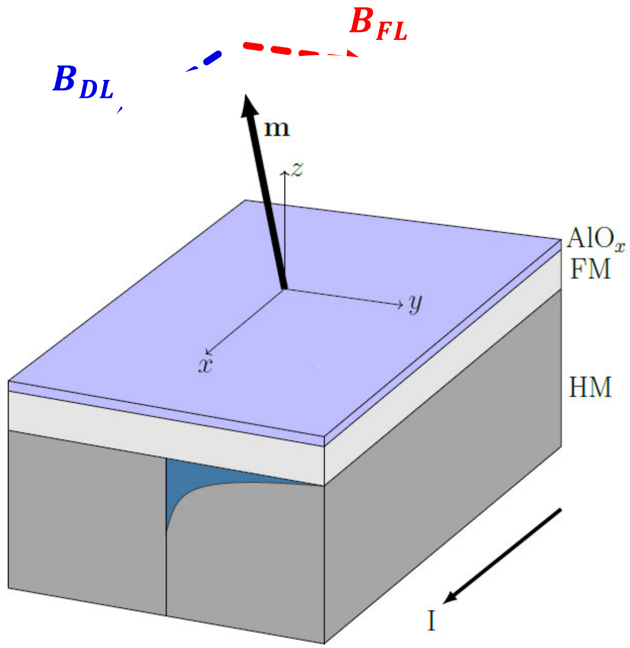

Spin/orbital accumulation
due to interfacial Rashba-Edelstein effect

Manchon, PG et al., Rev. Mod. Phys. **91**, 035004 (2019)

ETH zürich

Harmonic Hall voltage measurements of spin-orbit torques

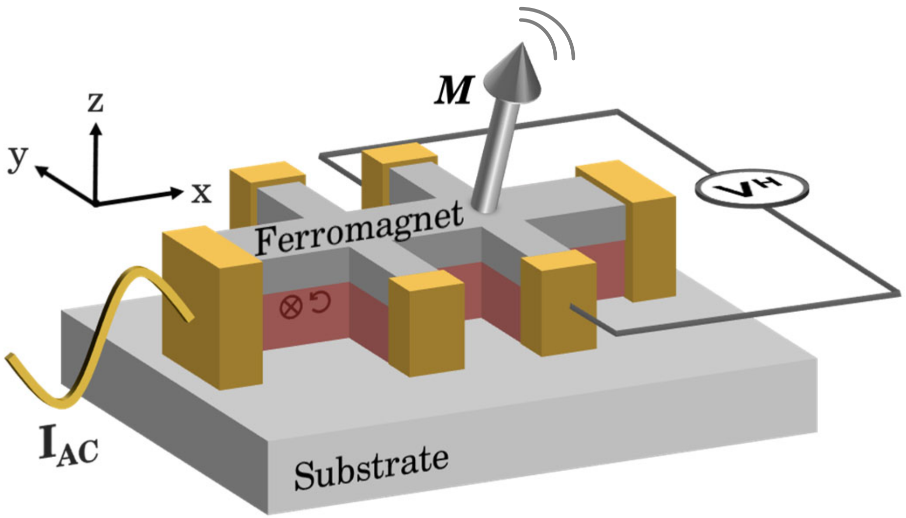

Out-of-plane magnetization:
Garello, PG et al., *Nat. Nanotech* **8**, 587 (2013)
Ghosh, PG et al., *Phys. Rev. Appl.* **7**, 014004 (2017)
Hayashi et al., *Phys. Rev. B* **89**, 144425 (2014)

In-plane magnetization:
Avci, PG et al. *Phys. Rev. B* **90**, 224427 (2014)
Noël, PG et al, *Phys. Rev. B* **111**, 144409 (2025)

$$R_{xy}^{2\omega}(\varphi) = R_{\mathrm{PHE}}\left(2\cos^3\varphi - \cos\varphi\right)\frac{B_{\mathrm{FL}} + B_{\mathrm{Oe}}}{B_{\mathrm{ext}}} + \left(\frac{1}{2}R_{\mathrm{AHE}}\frac{B_{\mathrm{DL}}}{B_{\mathrm{ext}} + B_{\mathrm{anis}}} + R_{\nabla T}\right)\cos\varphi$$

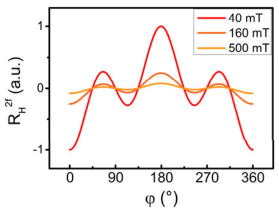

FL torque leads to oscillation of ***M*** in the plane: change of PHE

$$\xi_{\mathrm{FL}}^{\mathrm{E}} = \frac{2e}{\hbar} M t_{\mathrm{FM}} \frac{B_{\mathrm{FL}}}{E}$$

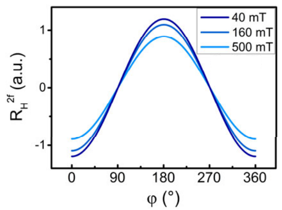

DL torque leads to oscillation of ***M*** out of plane: change of the AHE

$$\xi_{\mathrm{DL}}^{\mathrm{E}} = \frac{2e}{\hbar} M t_{\mathrm{FM}} \frac{B_{\mathrm{DL}}}{E}$$

Orbital torques in three steps

ETH zürich

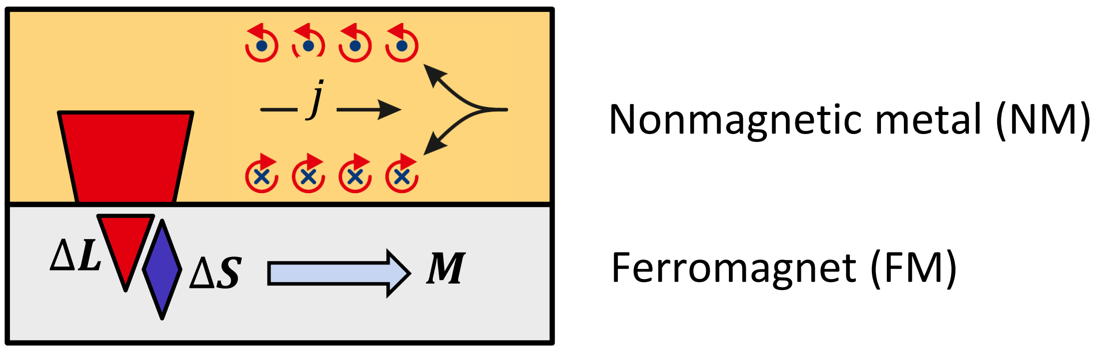

1. **Generation** of nonequilibrium orbital current and/or orbital accumulation
2. **Injection** of orbital current into the FM
3. **Conversion** of the orbital current to a spin current and spin torque $\boldsymbol{T} \sim \Delta\boldsymbol{S}/\Delta t$

D. Go et al., Phys. Rev. Res. **2**, 013177 & 033401 (2020)
G. Sala and PG, Phys. Rev. Res. **4**, 033037 (2022)

Can we distinguish between spin and orbital torques?

ETH zürich

The periodic table method
(handle with care)

3*d*
4*d*
5*d*

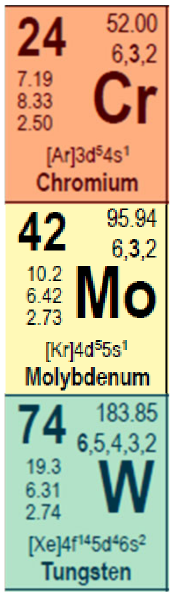

Mostly Orbital

One or the other

Mostly Spin

Ti/Ni,NiFe Hayashi et al., Comm. Phys. **6**:32 (2023)
Ti/CoFeB Choi et al., Nature **619**, 52 (2023)
Cr/Ni,Co Lee et al., Comm. Phys. **4**, 234 (2021)
Mn,Cr/Ni,Co Sala and PG, PRR **4**, 033037 (2022)
Cr/CoFeB Chiba et al., Nao Lett. **24**, 14028 (2024)
Zr/CoFeB Zheng et al., PRR 2, 13127 (2020)

CuOx/NiFe An et al., Nat. Comm. **7**, 13069 (2016)
Gao et al., PRL **121**, 17202 (2018)
CuOx/Co,CoFe Ding et al., PRR 4, L032041 (2022)
Damerio and Avci, Nano Lett. **25**, 2181 (2025)
Ox/Cu/CoFe Kim et al., PRB **103**, L020407 (2021)
Ox/Cu/Pt Krishmia et al., APL Mater. **12**, 051105 (2024)

Nb/Ni,NiFe Dutta and Tulapurkar, PRB **106**, 184406 (2022)
Nb,Ru/Ni,CoFeB Bose et al., PRB **107**, 134423 (2023)

…

Control of L-S conversion in orbital torque systems

ETH zürich

by FM layer

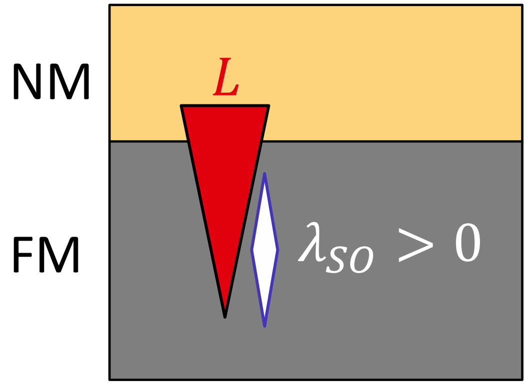

weak L-S conversion

by spacer layer

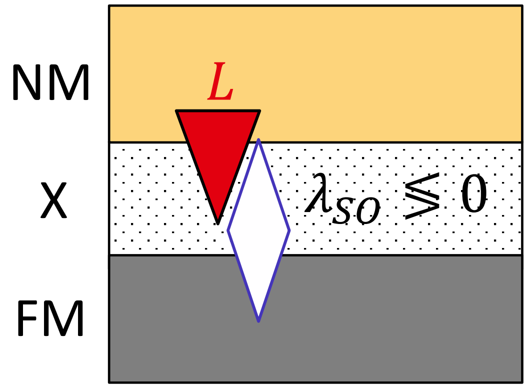

large L-S conversion

X=Pt, Gd, Tb,…

Lee et al., Comm. Phys. **4**, 234 (2021)
Lee et al., Nat. Comm. **12**, 6710 (2021)
Sala and PG, Phys. Rev. Res. **4**, 033037 (2022)

Ding et al., PRL **125**, 177201 (2020)
Sala and PG, PRR **4**, 033037 (2022)

Evidence of orbital-to-spin conversion from orbital torque measurements

ETH zürich

Opposite torques produced by light-metal Cr in Ni and Co

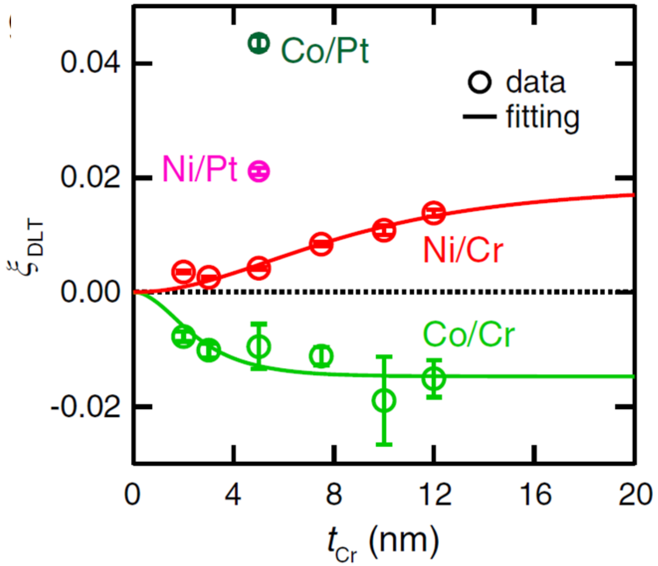

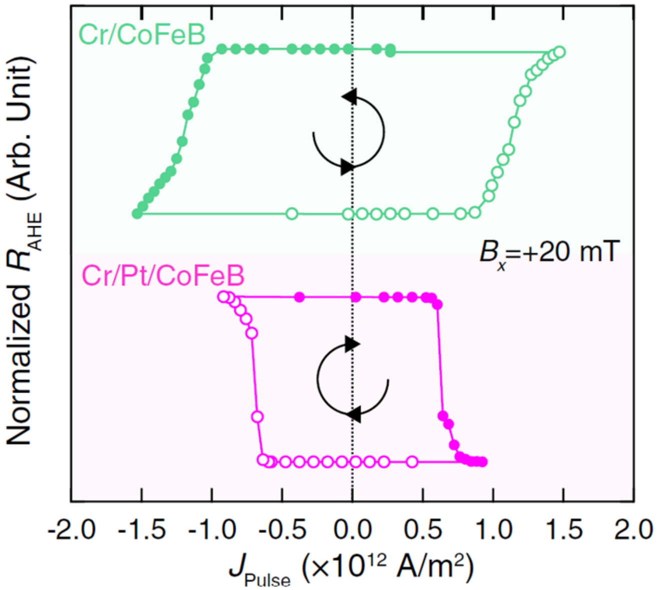

Lee et al., Comm. Phys. **4**, 234 (2021)
Sala and PG, Phys. Rev. Res. **4**, 033037 (2022)

Enhancement of torque upon insertion of 1-nm-thick Pt between CuOx and TmIG

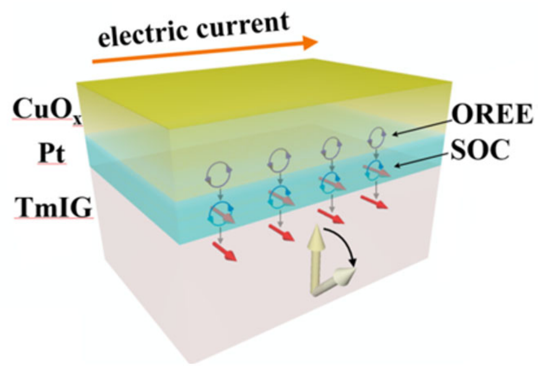

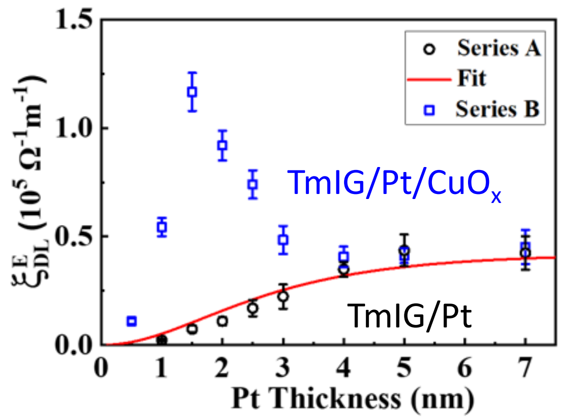

Ding et al., PRL **125**, 177201 (2020)

Giant orbital-to-spin conversion by 4f metal spacers

ETH zürich

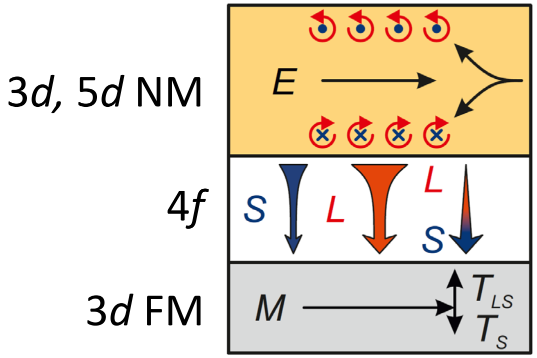

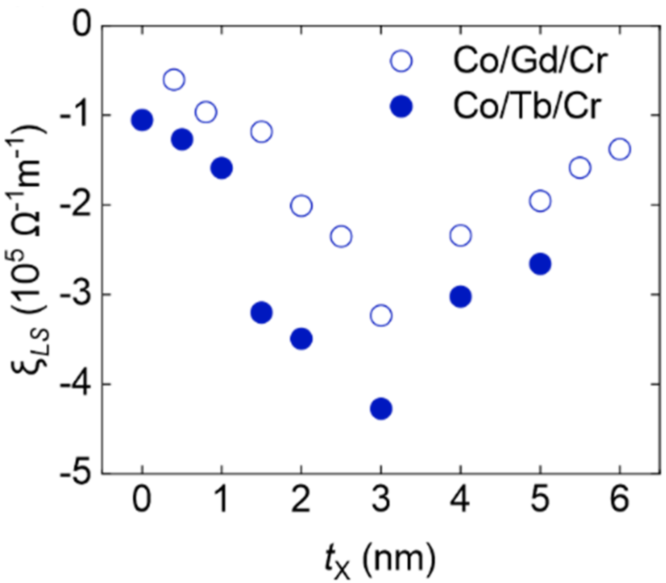

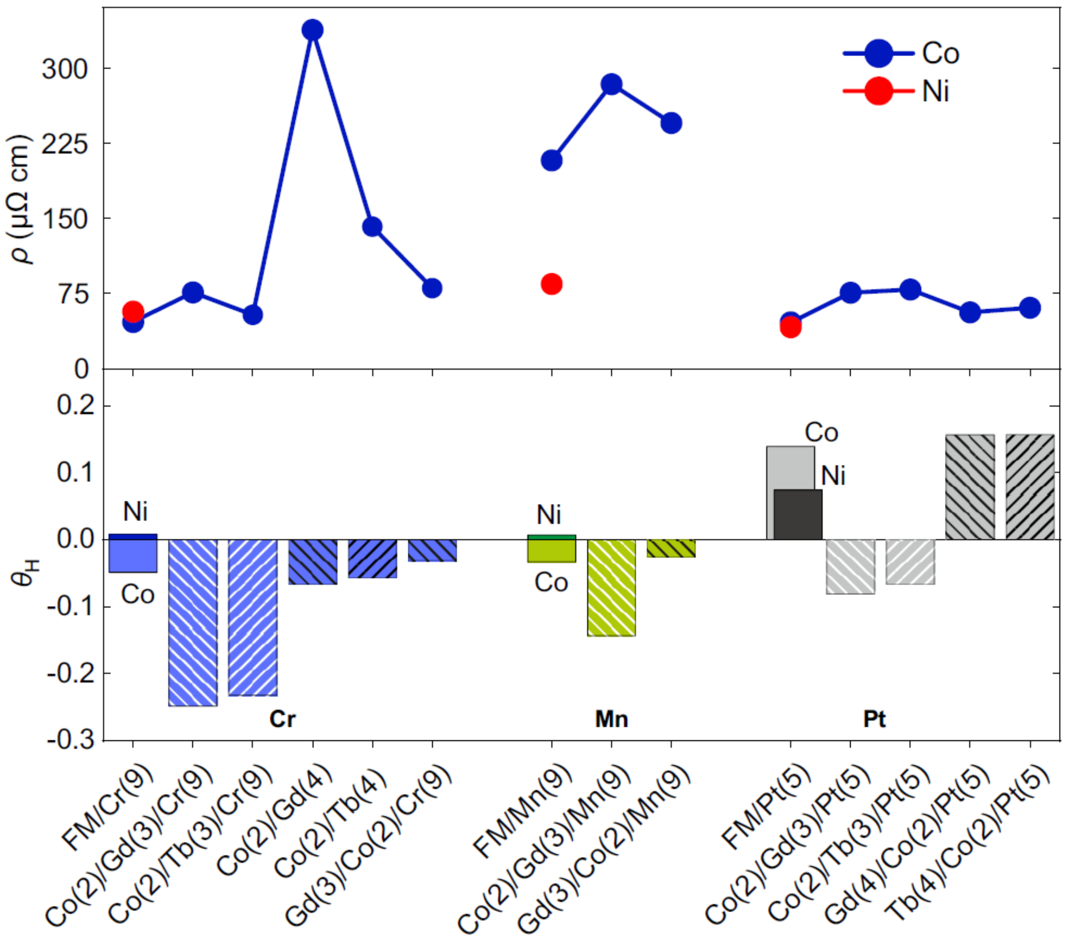

G. Sala and PG, Phys. Rev. Res. **4**, 033037 (2022)

Coexistence of orbital Hall and spin Hall effects in Pt

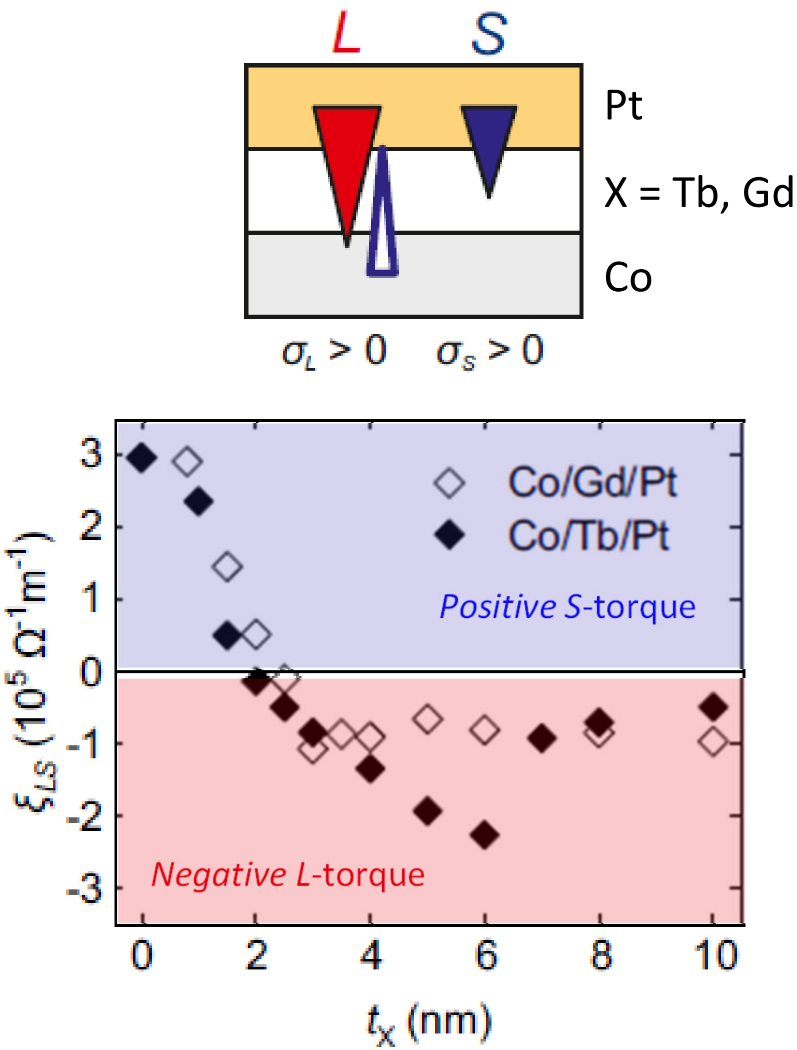

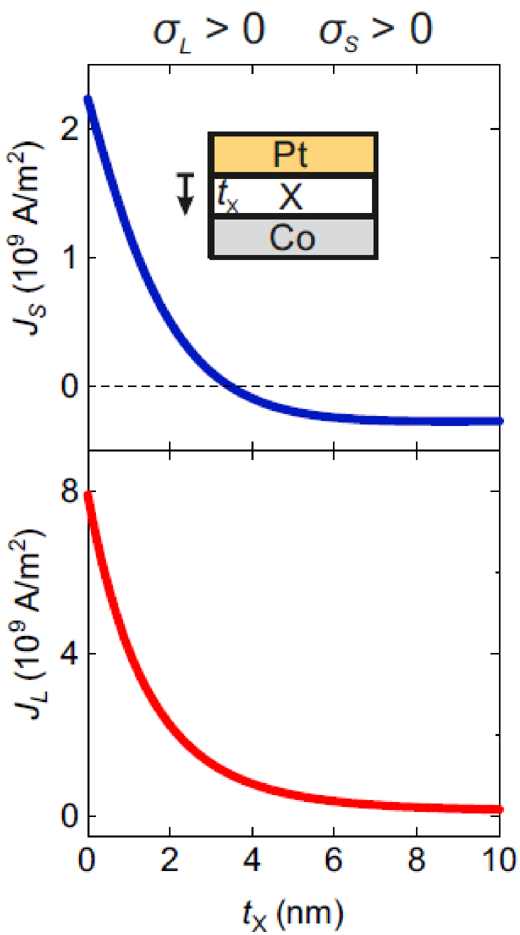

L-S coupled
drift-diffusion model

$$j_S = -\frac{\sigma}{2e}\frac{d\mu_S}{dz} + \sigma_S E,$$

$$j_L = -\frac{\sigma}{2e}\frac{d\mu_L}{dz} + \sigma_L E,$$

$$\frac{d^2\mu_S}{dz^2} = \frac{\mu_S}{\lambda_S^2} \pm \frac{\mu_L}{\lambda_{LS}^2}$$

$$\frac{d^2\mu_L}{dz^2} = \frac{\mu_L}{\lambda_L^2} \pm \frac{\mu_S}{\lambda_{LS}^2},$$

G. Sala and PG, Phys. Rev. Res. **4**, 033037 (2022)

Control of L-S conversion in orbital torque systems

ETH zürich

by FM layer

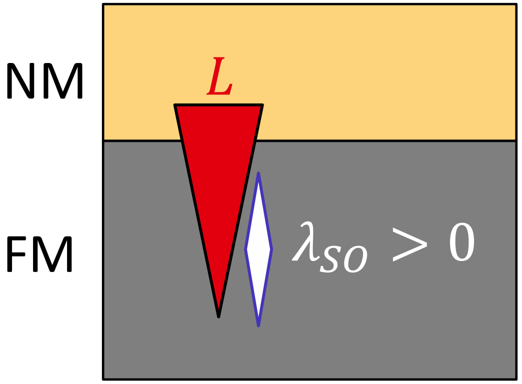

weak L-S conversion

by spacer layer

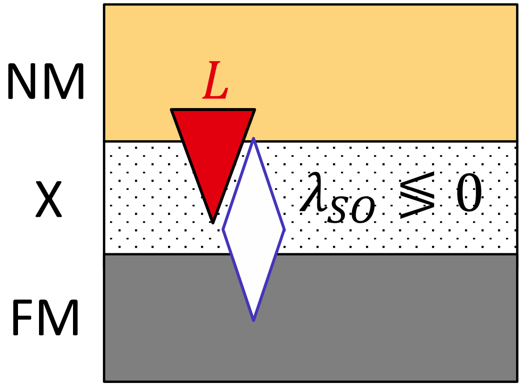

large L-S conversion

X=Pt, Gd, Tb,…

by FM alloy

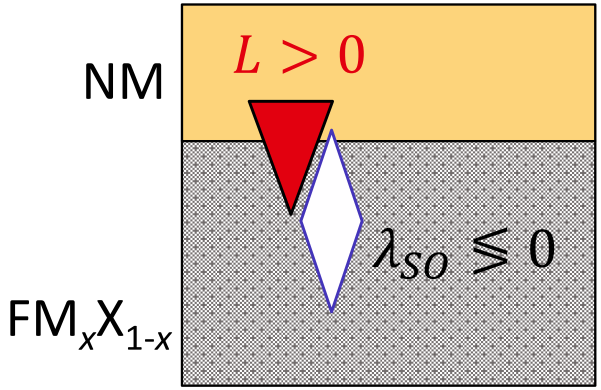

tunable L-S conversion

Lee et al., Comm. Phys. **4**, 234 (2021)
Lee et al., Nat. Comm. **12**, 6710 (2021)
Sala and PG, Phys. Rev. Res. **4**, 033037 (2022)

Ding et al., PRL **125**, 177201 (2020)
Sala and PG, PRR **4**, 033037 (2022)

Ding, PG et al. PRL **132**,236702 (2024)

Cu/CuOx: a source of orbital torque

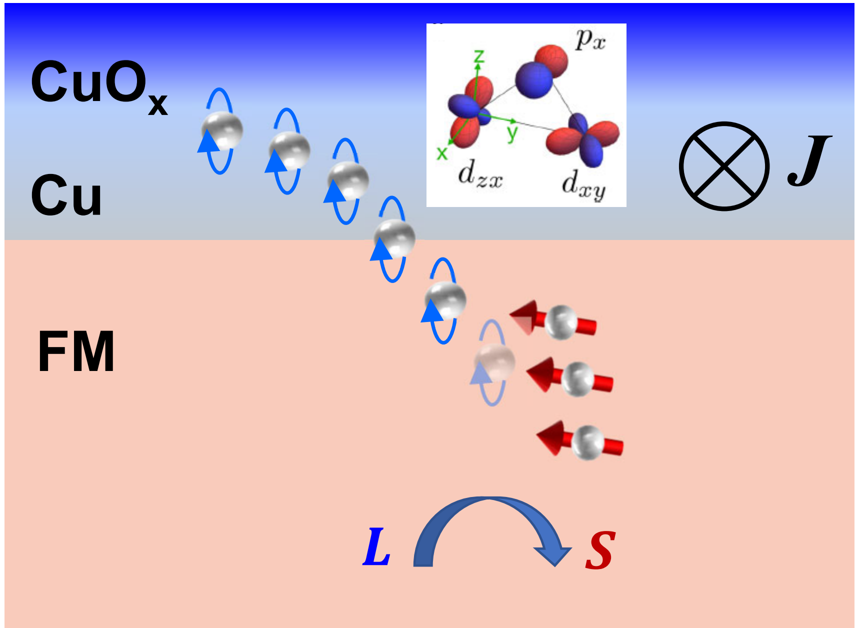

An et al., Nat. Comm. **7**, 13069 (2016)
Gao et al., Phys. Rev. Lett. **121**, 017202 (2018)

Orbital Rashba-Edelstein effect at the Cu/CuOx interface:
Go et al., Phys. Rev. B, **103**, L121113 (2021)

Electron vorticity at the Cu/CuOx interface:
Yi et al., Phys. Rev. Lett., **135** 156702 (2025)

Orbital *vs* spin injection in a RE-TM ferrimagnet

Orbital injection

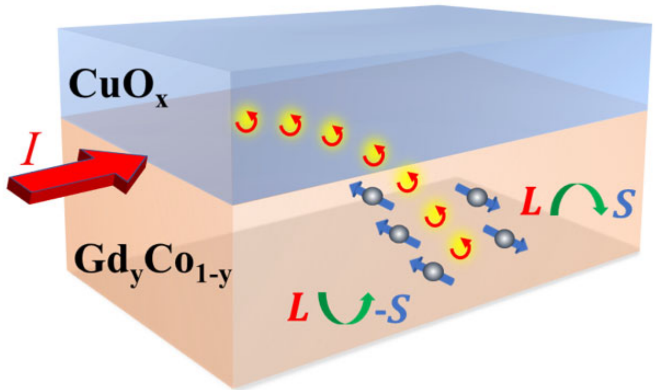

Spin injection

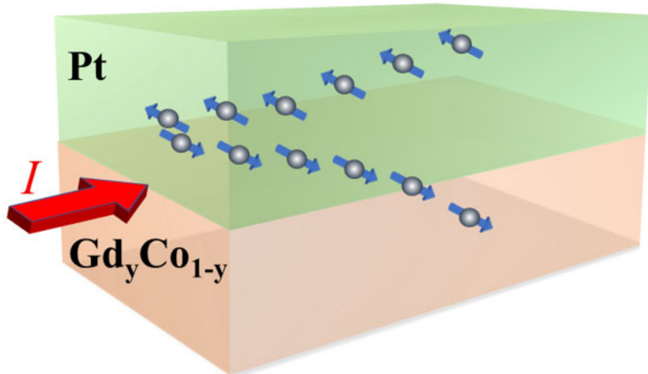

Ding, PG et al. Phys. Rev. Lett. **132**,236702 (2024)

Orbital-to-spin conversion in $Gd_yCo_{y\text{-}100}/CuO_x$

ETH zürich

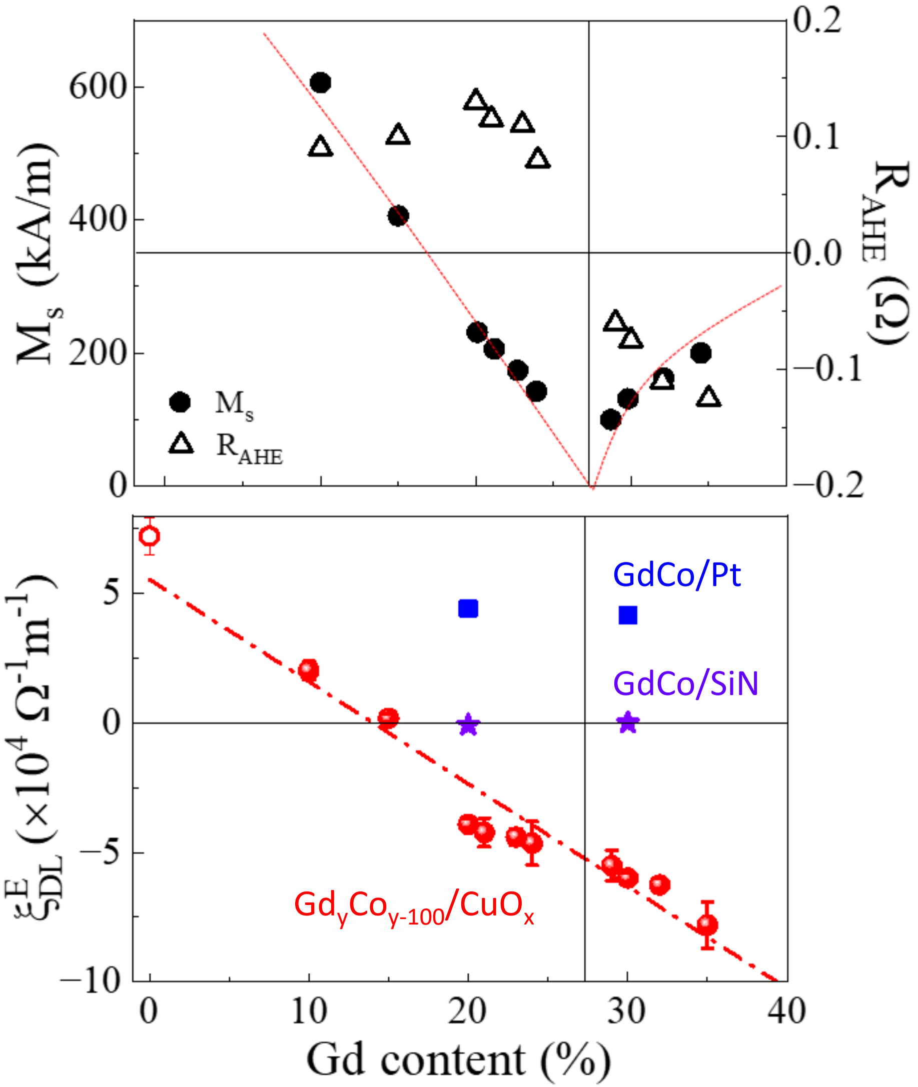

- Magnetic compensation point at 27% Gd
- Torque compensation point at 15% Gd.
- Linear scaling of $\xi_{\mathrm{DL}}^{\mathrm{E}}$ with Gd%

$$\xi_{\mathrm{DL}}^{\mathrm{E}} = \frac{2e}{\hbar}\sigma_{\mathbf{L}}^{\mathrm{CuOx}}\left[\frac{y}{100}\eta_{\mathrm{L\cdot S}}^{\mathrm{Gd}} + \frac{100-y}{100}\eta_{\mathrm{L\cdot S}}^{\mathrm{Co}}\right]$$

- Efficiency of L-S conversion

$$\frac{\left|\eta_{\mathrm{L\cdot S}}^{\mathrm{Gd}}\right|}{\left|\eta_{\mathrm{L\cdot S}}^{\mathrm{Co}}\right|} \approx 5 \approx \frac{\lambda_{so}^{\mathrm{Gd}}}{\lambda_{so}^{\mathrm{Co}}} = \frac{250\ \mathrm{meV}}{60\ \mathrm{meV}}$$

Lacueva, Levy, Fert,
PRB **26**, 1099 (1982);
Sol. St. Comm. **38**, 551 (1981)

Ding, PG et al. Phys. Rev. Lett. **132**,236702 (2024)

Orbital-to-spin conversion in Gd_yCo_{y-100}/CuO_x: temperature dependence

ETH zürich

Effective SH angle

$\xi^{j}_{DL} = +0.13$

$\xi^{j}_{DL} = +0.03$

$\xi^{j}_{DL} = -0.25$

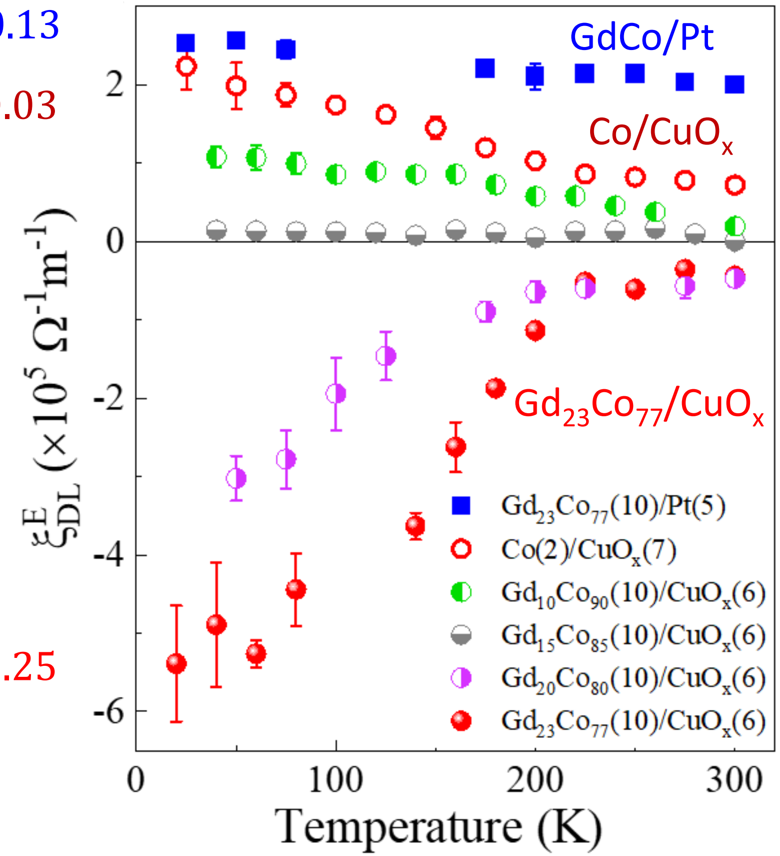

$Co(2)/CuO_x(7)$
x 3 increase
consistent
with OREE

$Gd_{23}Co_{77}(10)/CuO_x(6)$
x 12 increase

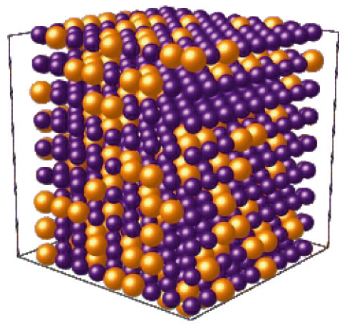

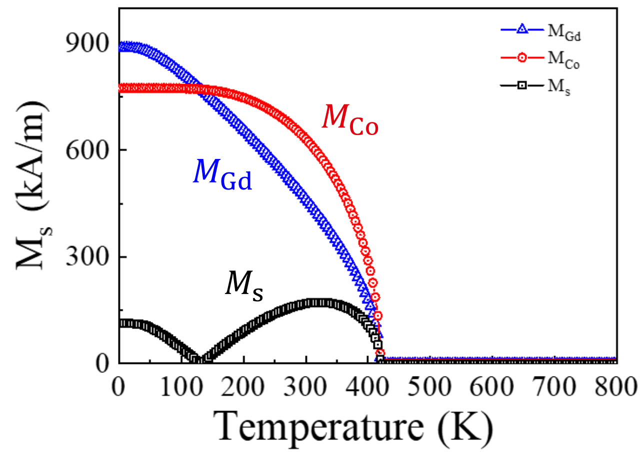

$$\xi^{E}_{DL} \sim M_{Gd,Co}(T)$$

S. Ding, PG et al. Phys. Rev. Lett. **132**,236702 (2024)

L-S conversion in antiferromagnets

by FM layer

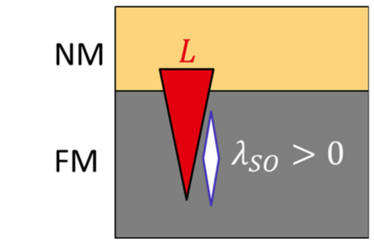

by spacer layer

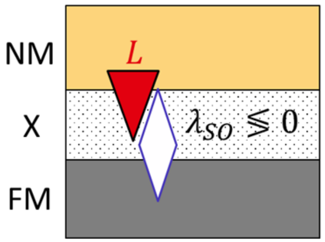

by FM alloy

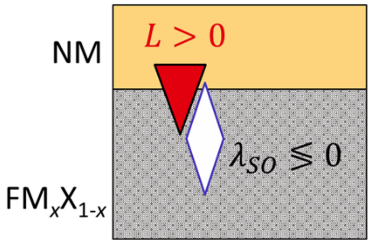

by antiferromagnets ?

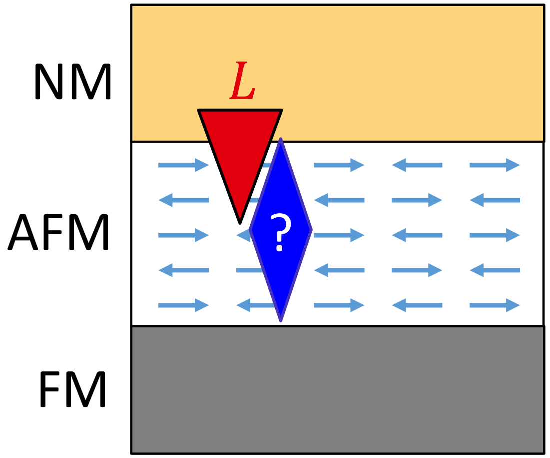

Spin transport in insulating AFMs

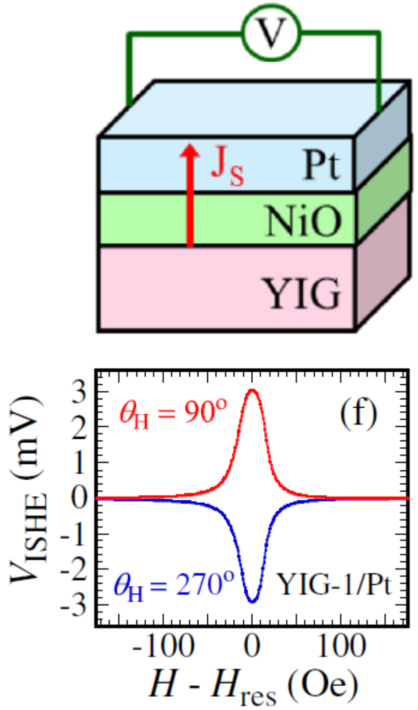

Spin pumping:
Wang et al.,
PRL 113, 97202 (2014)
Hahn et al.,
EPL 108, 57005 (2014)

Spin-orbit torques:
Zhu et al., PRL 126, 107204 (2021)

Magnon-mediated switching:
Wang et al., Science 366, 1125 (2019)

Spin transport in insulating antiferromagnets

ETH zürich

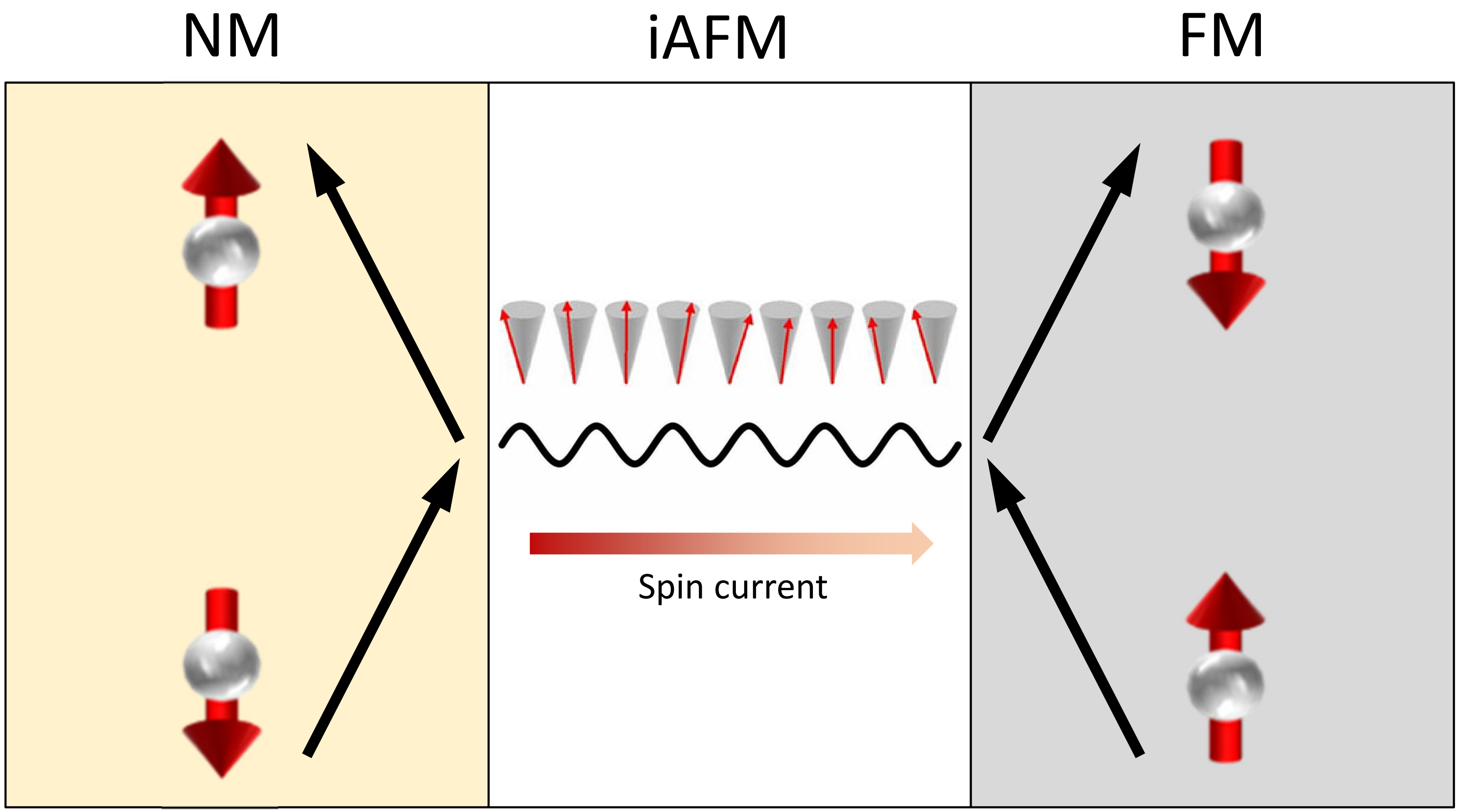

Orbital transport in insulating antiferromagnets ?

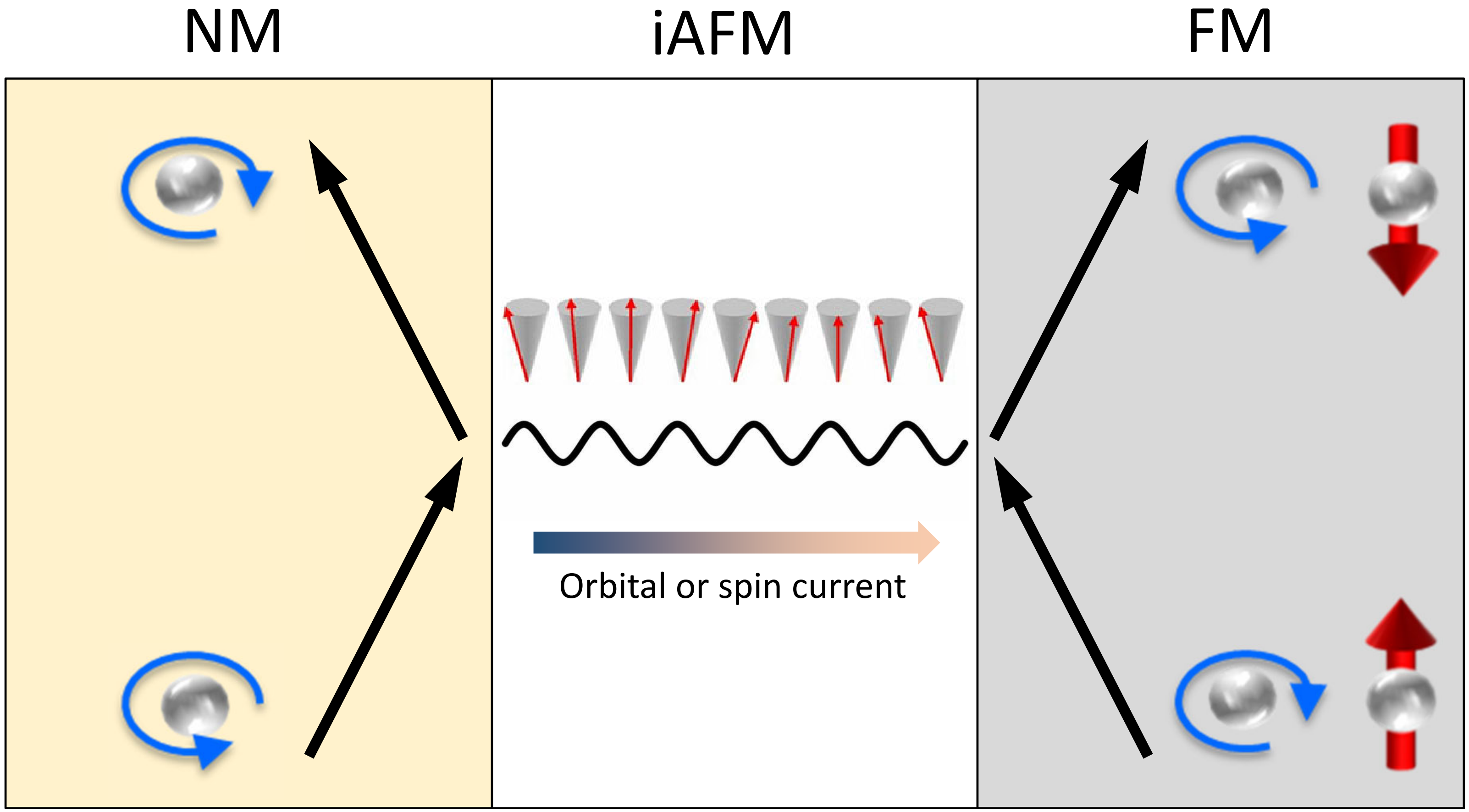

Orbital torques mediated by CoO

ETH zürich

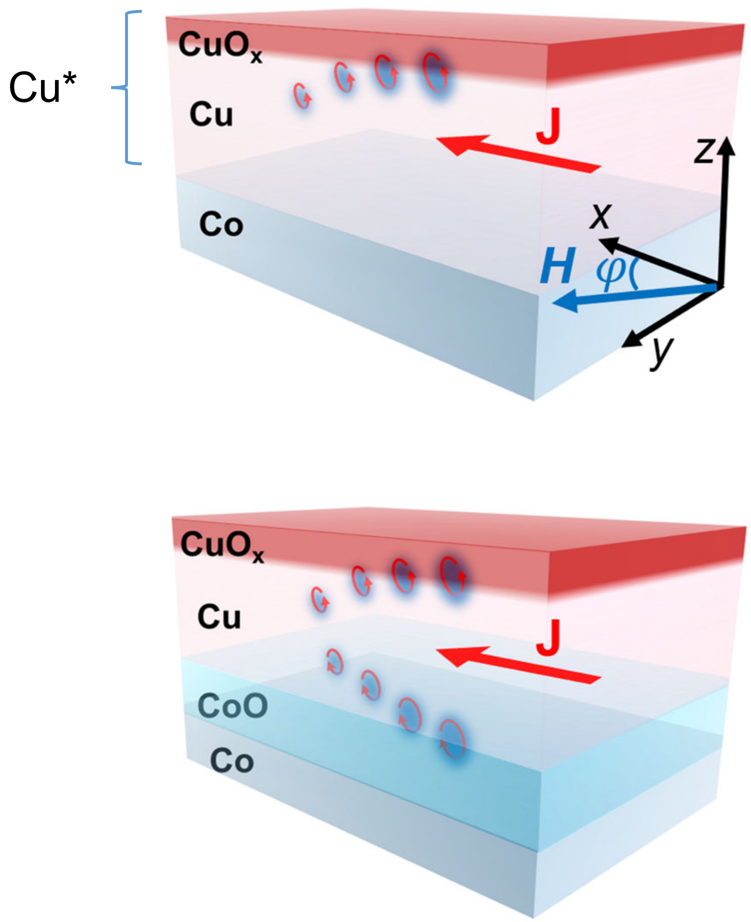

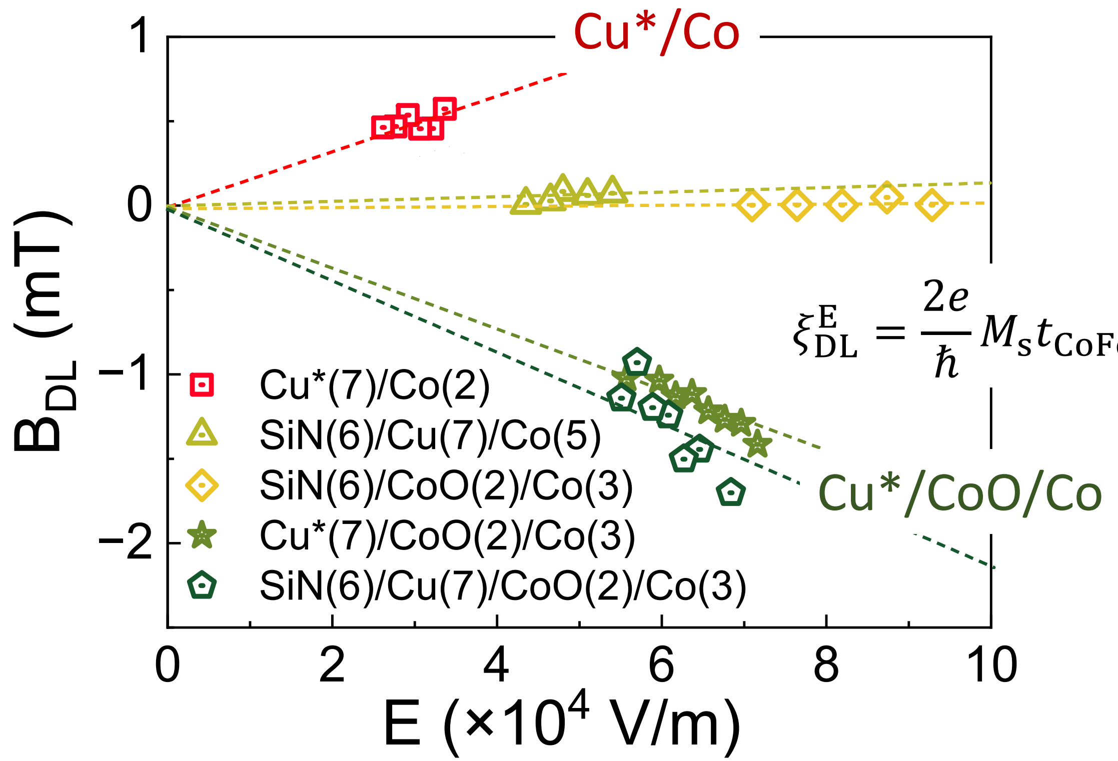

$$\xi_{DL}^{E} = \frac{2e}{\hbar} M_s t_{CoFe} \frac{B_{DL}}{E}$$

Ding, PG et al., Nat. Comm. **16**, 9239 (2025)

Orbital torques mediated by CoO

ETH zürich

Torque efficiency

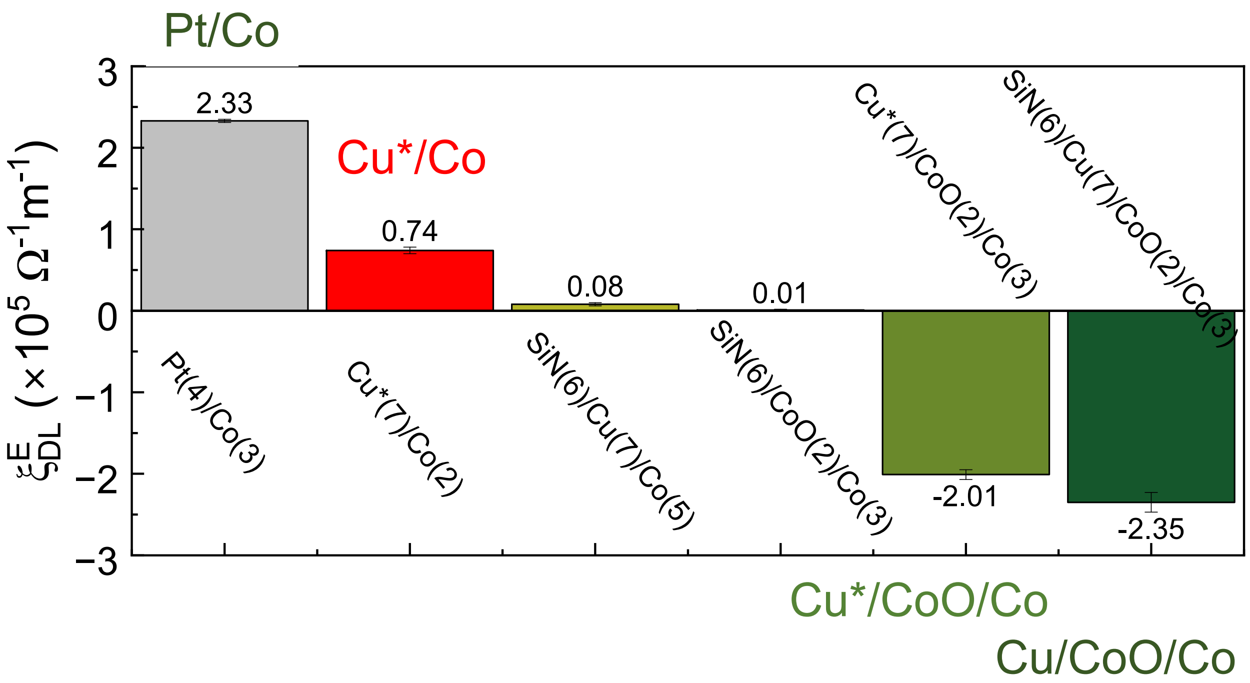

Thickness dependence

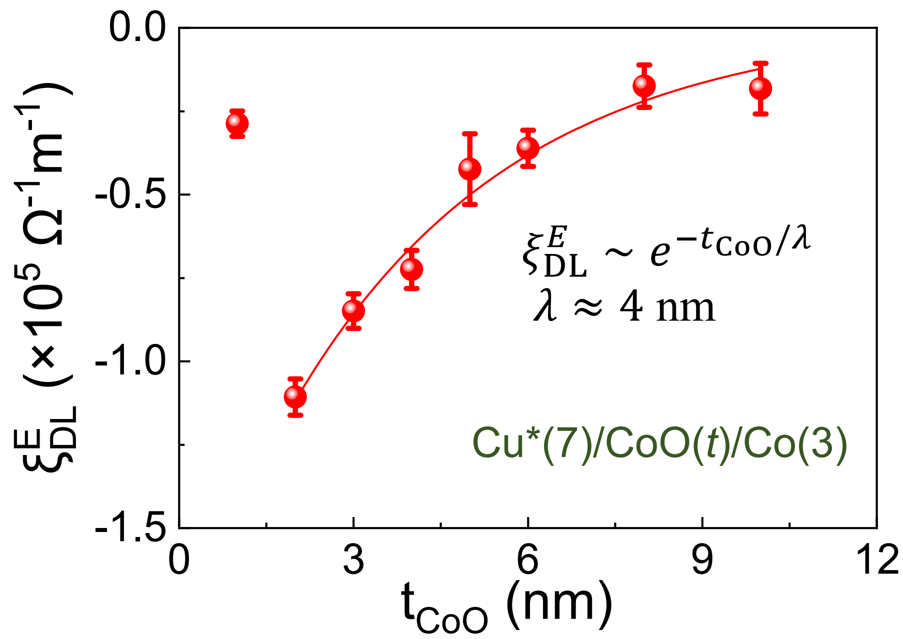

Ding, PG et al., Nat. Comm. **16**, 9239 (2025)

AFM transition and temperature dependence

ETHzürich

Cu*/Co

M *vs* H

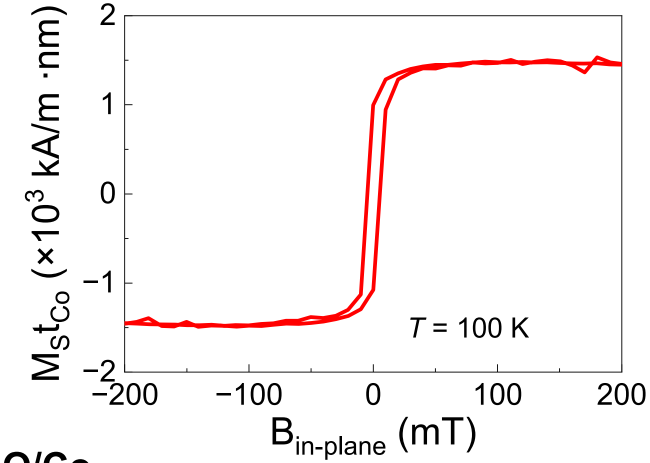

Exchange bias & coercivity

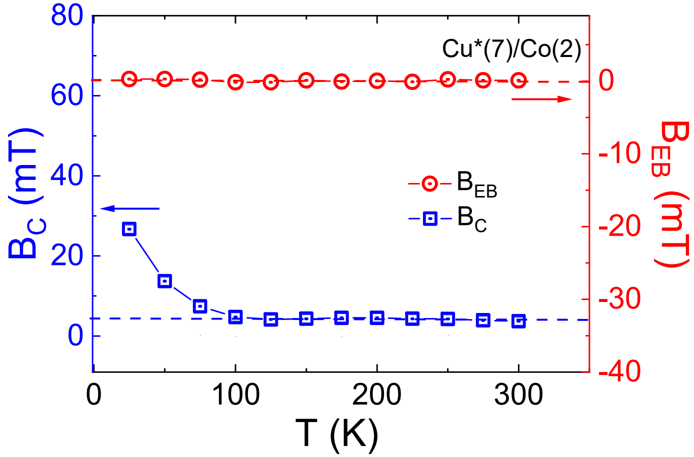

Temperature dependence of torque efficiency

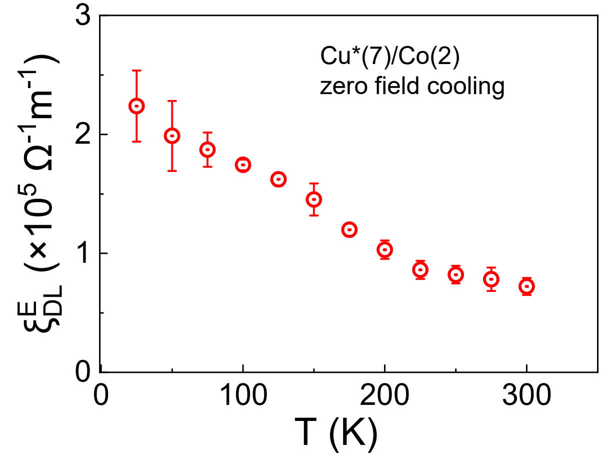

Cu*/CoO/Co

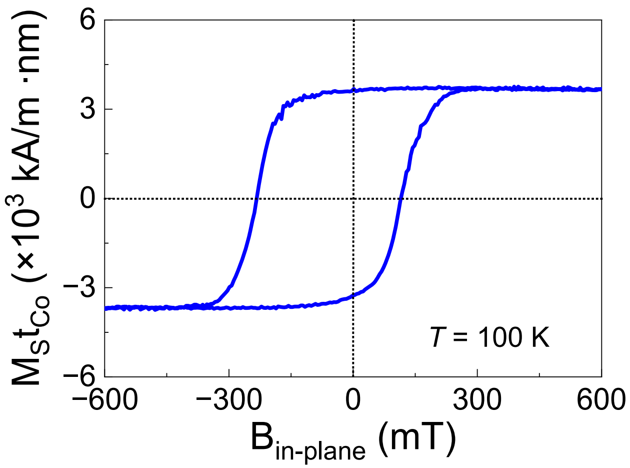

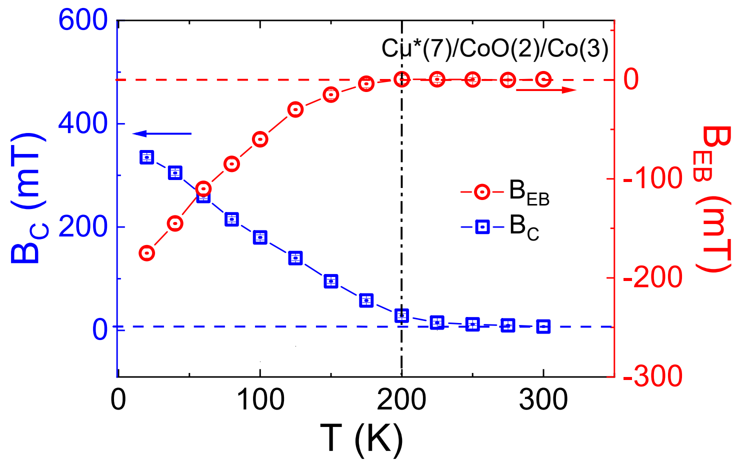

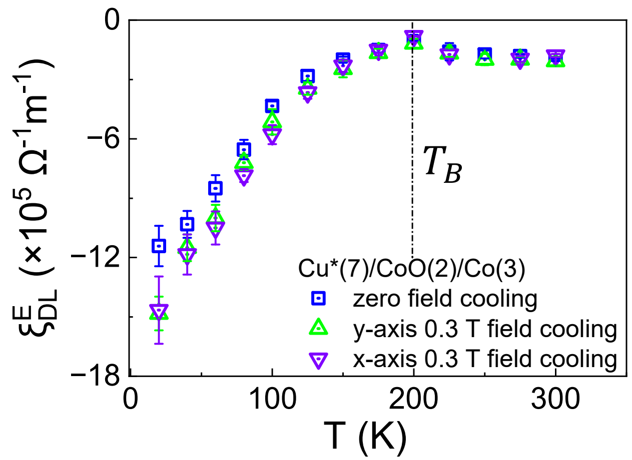

Spin-orbit excitons in CoO

Electronic ground state of Co^{2+}

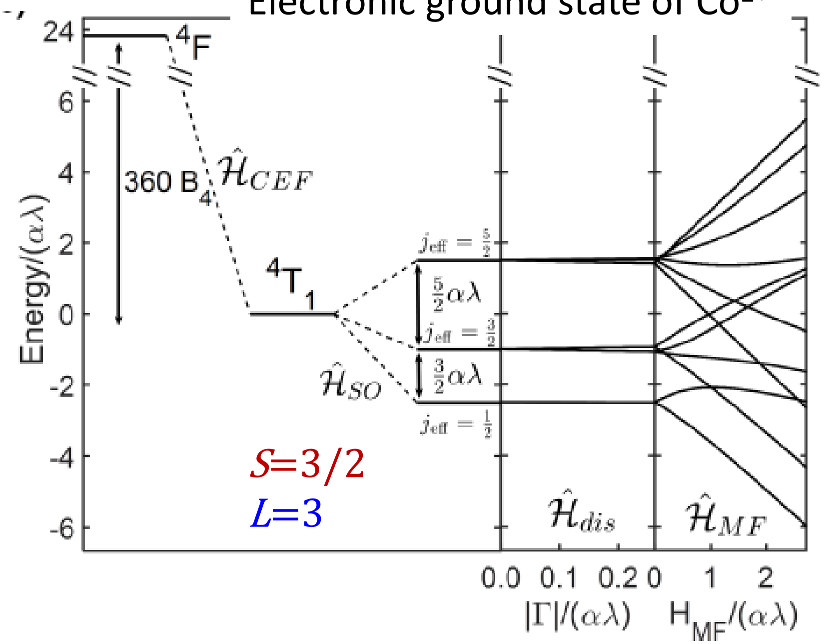

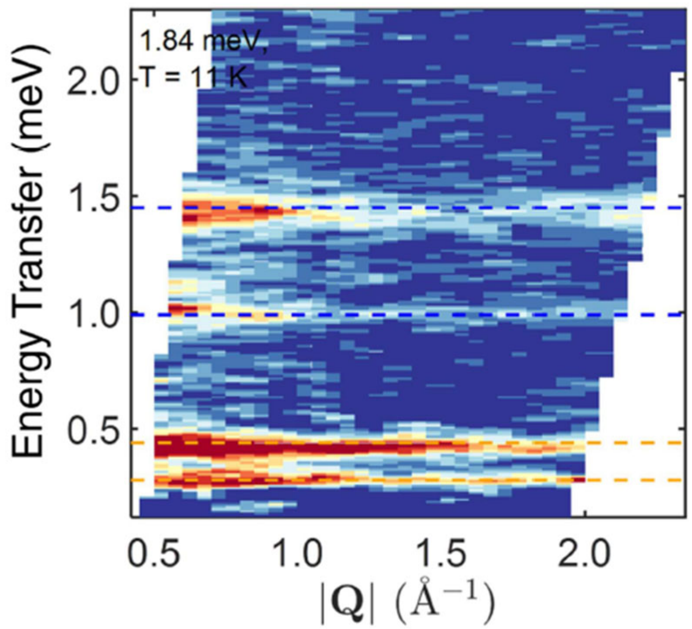

Low-energy magnetic excitation spectrum of Co^{2+} in $Mg_{0.97}Co_{0.03}O$

Sarte et al., Phys. Rev. B **100**, 075143 (2019); J. Phys. Cond. Matt. **32**, 374011 (2020)

Localized spin-orbit exciton

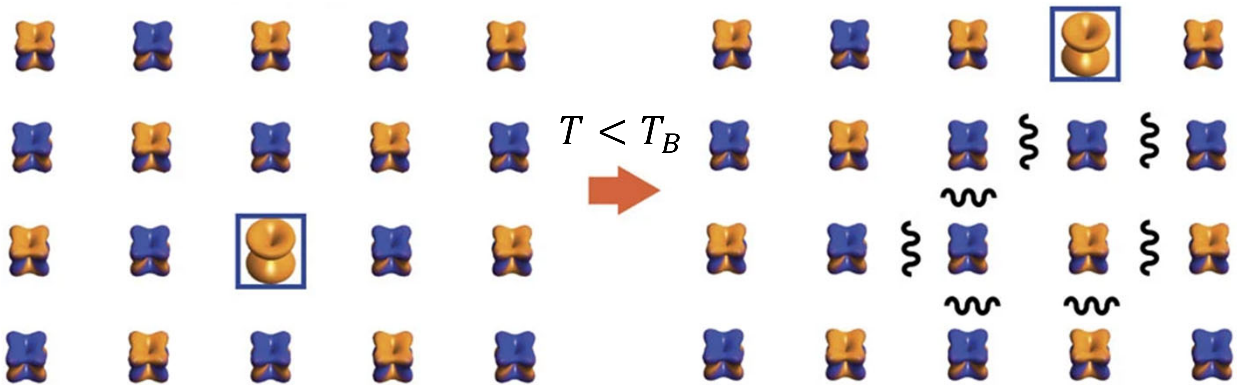

Propagating spin-orbit exciton dressed by magnons

J. Kim et al., Nat. Comm. **5**, 4453 (2014)

Scaling of orbital “transconductance” with orbital moments in CoO, NiO, MnO

ETH zürich

Damping-like torque
vs
applied *E*-field

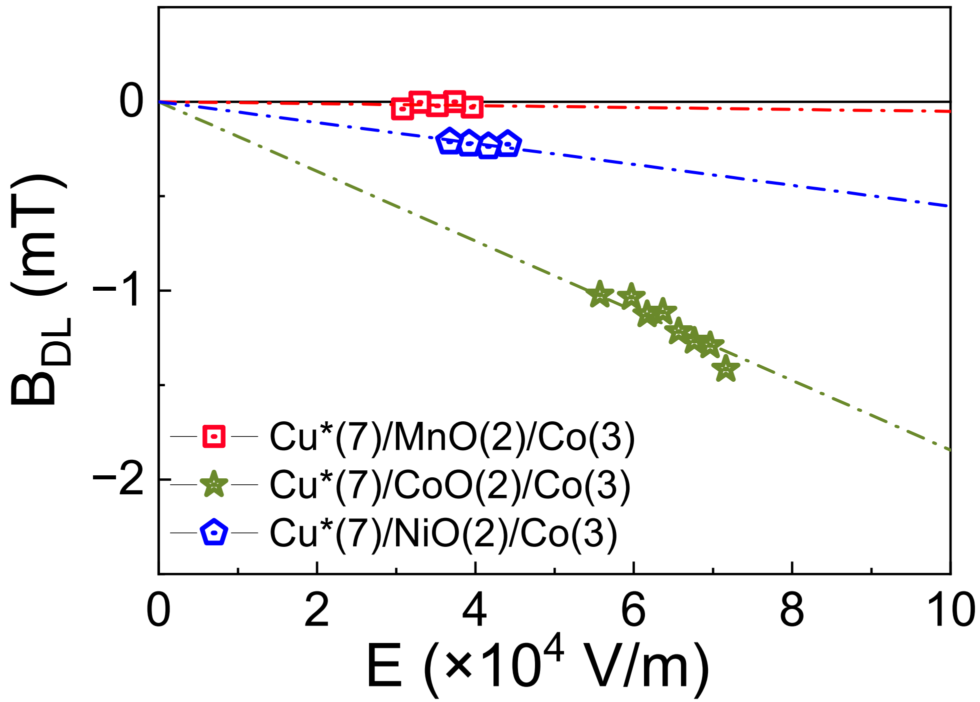

Torque efficiency
vs
orbital moment

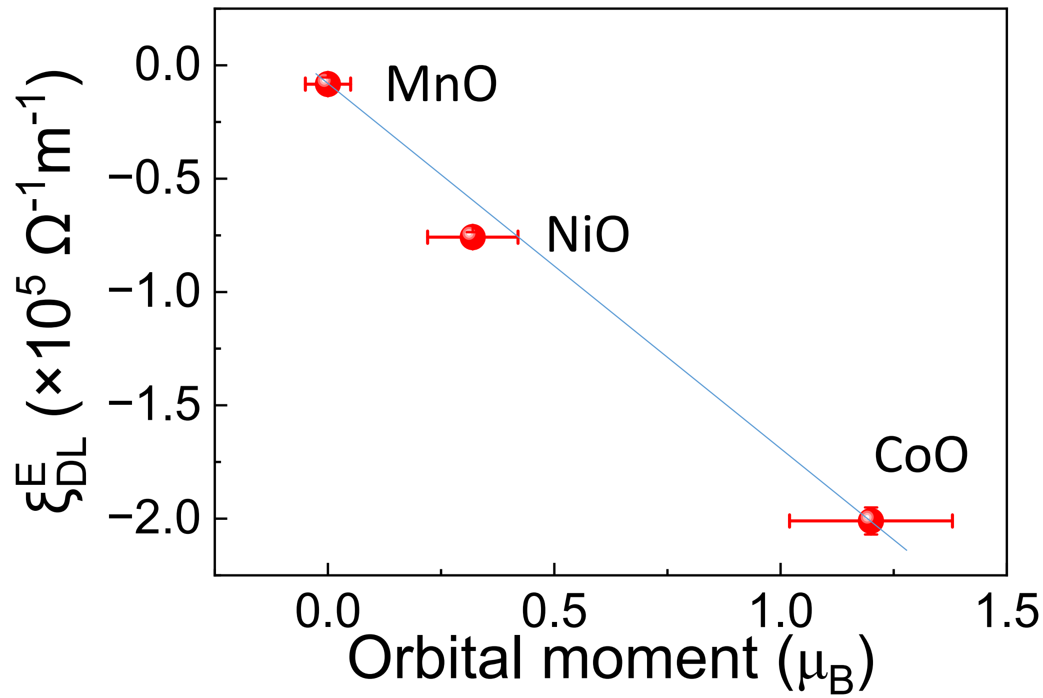

Ding, PG et al., Nat. Comm. **16**, 9239 (2025)

Summary of L-S conversion mechanisms

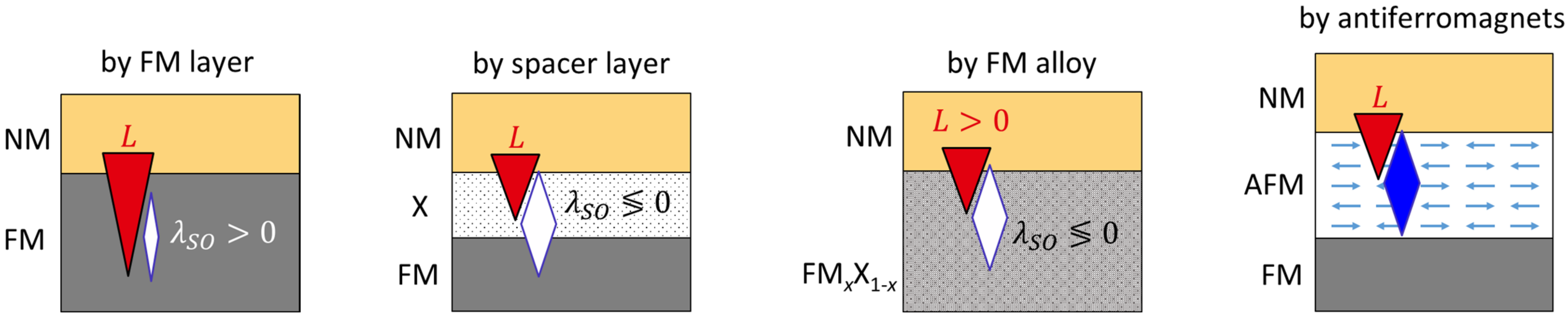

Applications of orbital torques in spintronic devices

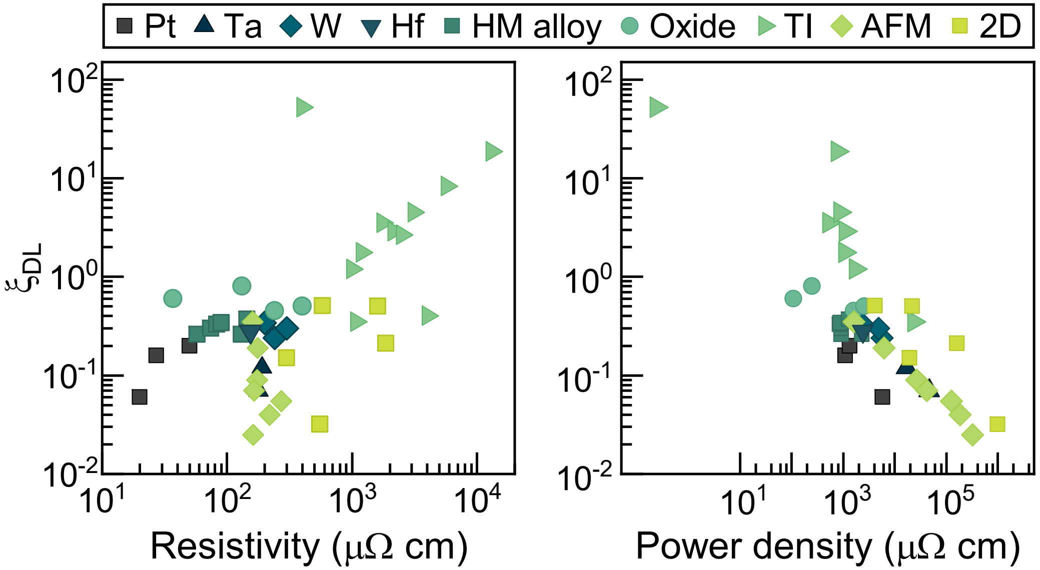

SOT efficiency

ξ_{DL}

Power efficiency

$$P_{SW} = j_{SW}^2 \rho \propto \frac{\rho}{\xi_{DL}^2}$$

Krizakova et al., *JMMM* **562**, 169692 (2022)
Zhu et al., *Appl. Phys. Rev*. **8**, 031308 (2021)

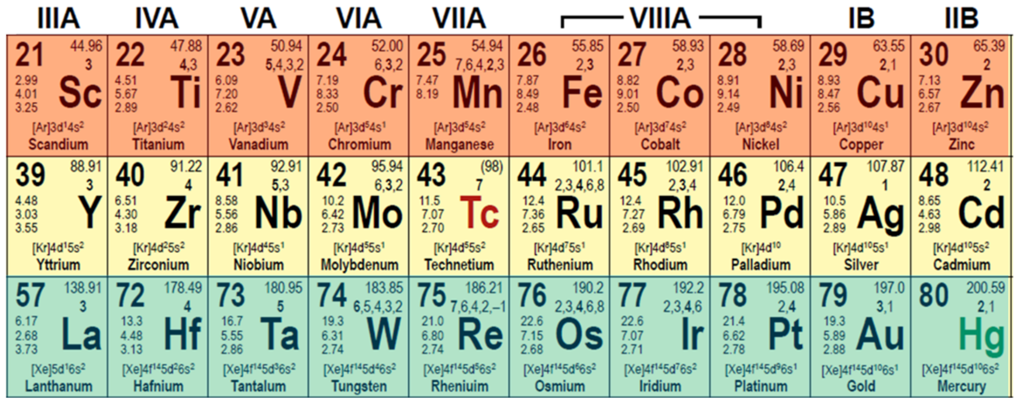

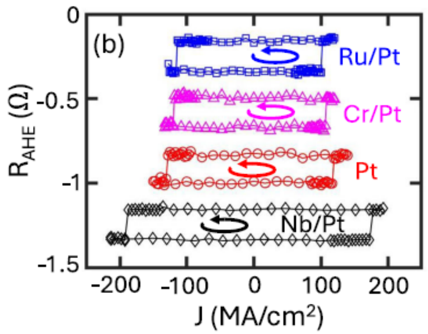

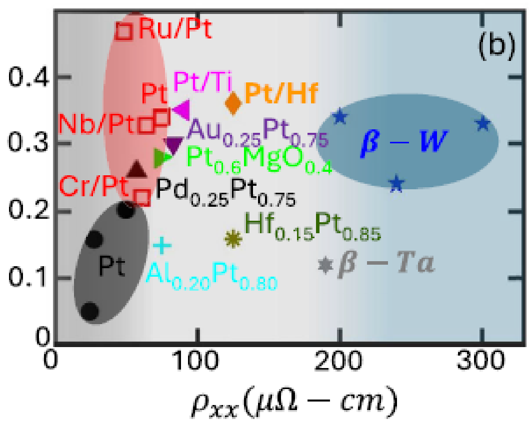

Gupta et al., *Nat. Comm*. **16**, 130 (2025)

Reciprocal S-L-charge conversion processes: Orbital pumping

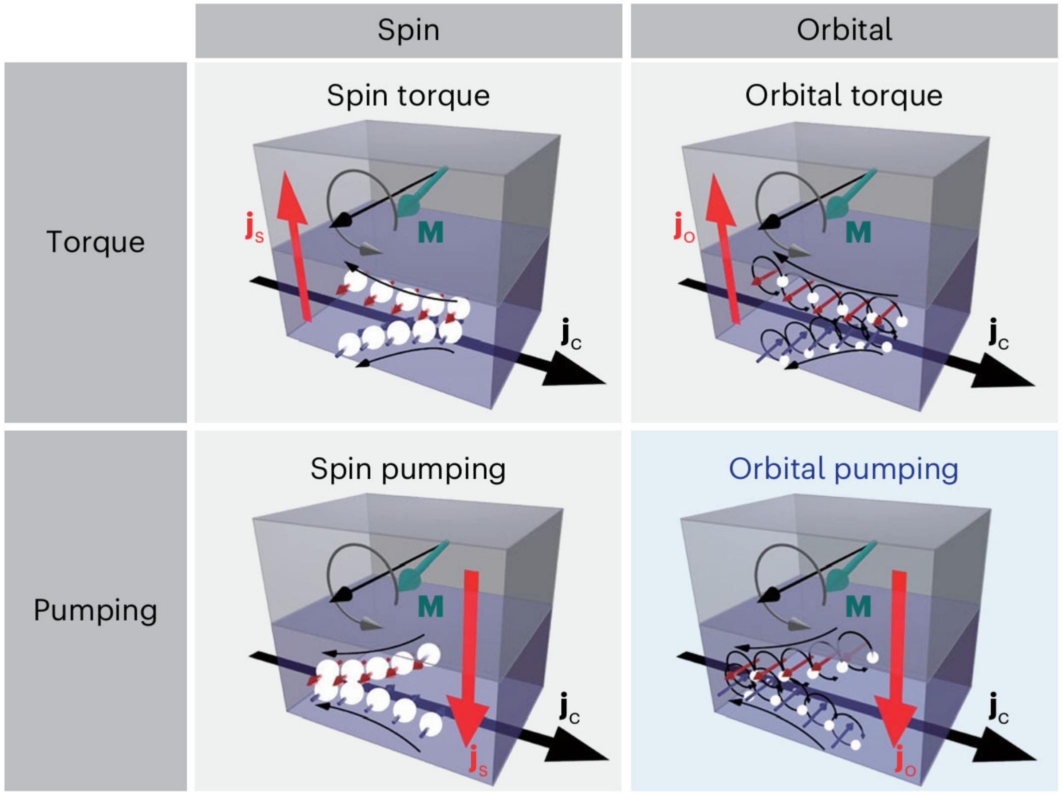

Hayashi et al., *Nat. Electron.* **7**, 646 (2024)

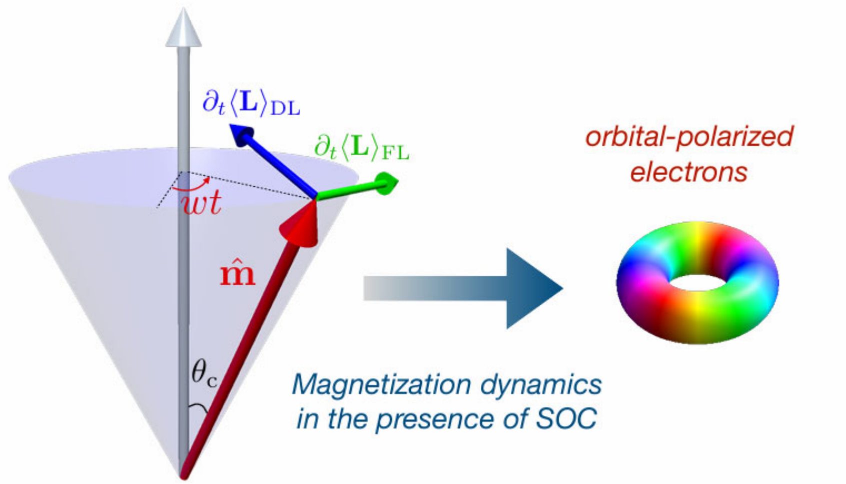

Theroy:
Go et al., *PRB* **111**, L140409 (2025)
Han et al., PRL **134**, 036305 (2025)

Experiments:
Santos et al., *PR Appl.* **19**, 014069 (2023)
El Hamdi et al., *Nat. Phys.* **19**, 1855 (2023)
Mondoza-Rodarte et al., *PRL* **132**, 226704 (2024)
Ledesma-Martin et al., *Nano Lett*. **25**, 3247 (2025)
Wang et al., *PRL* **134**, 126701 (2025)
...

g-factor scaling of orbital pumping from an insulating ferrimagnet into CuO_x

ETH zürich

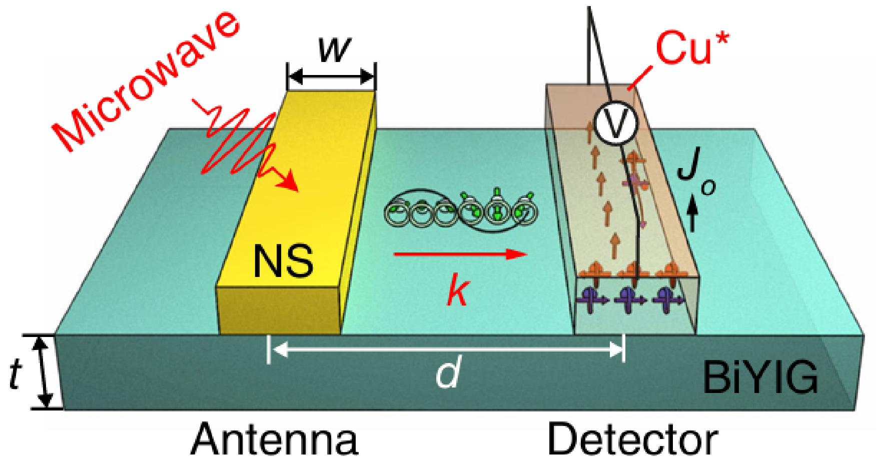

Charge generation efficiency

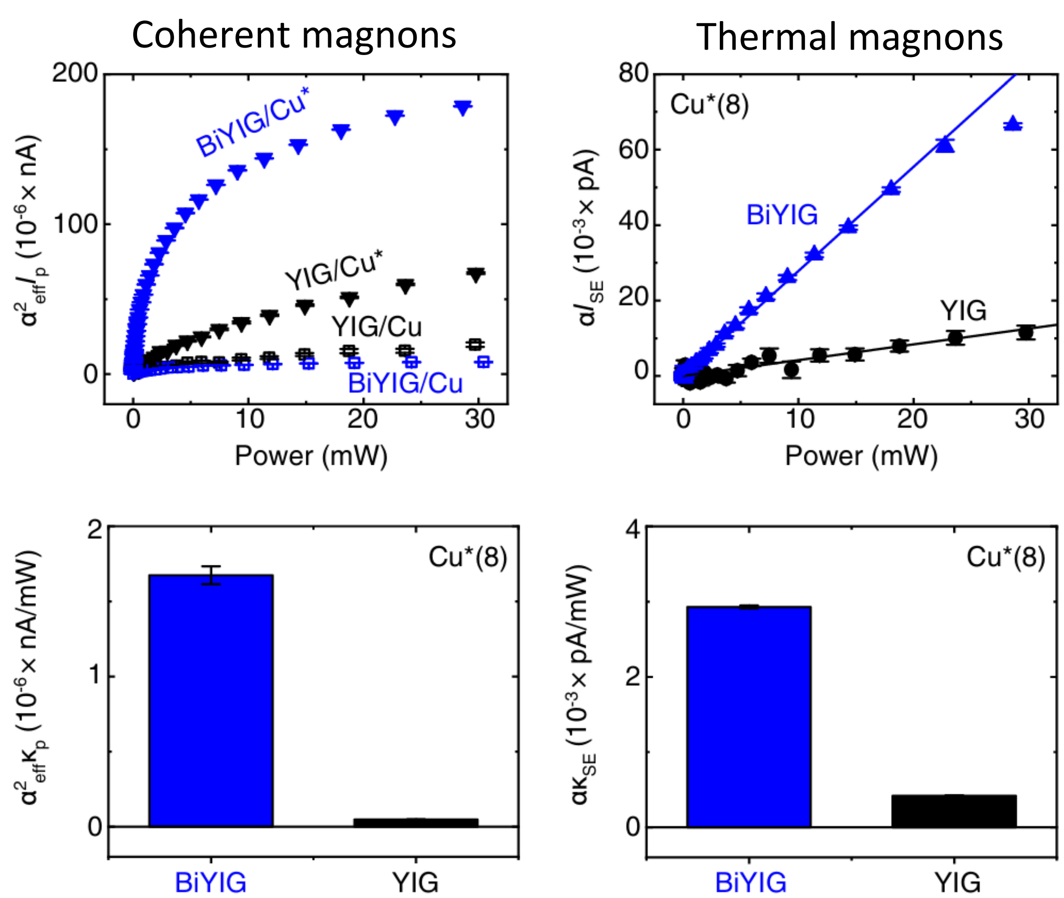

- BiYIG induces much larger orbital pumping than YIG
- Orbital pumping ratios are similar for coherent and thermal magnons
- Interfacial transparency matters

Wang et al., *PRL* **134**, 126701 (2025)

Reciprocal S-L-charge conversion processes: Orbital pumping

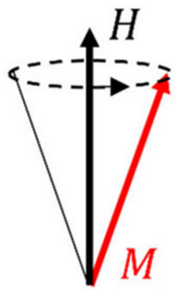

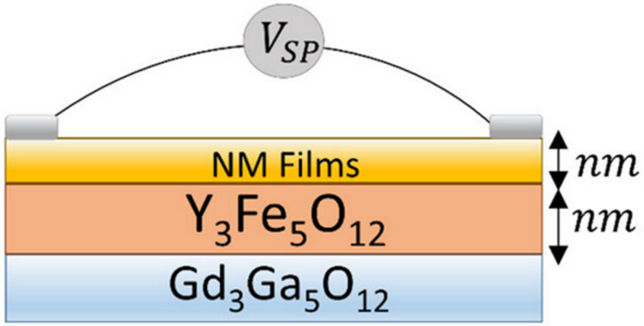

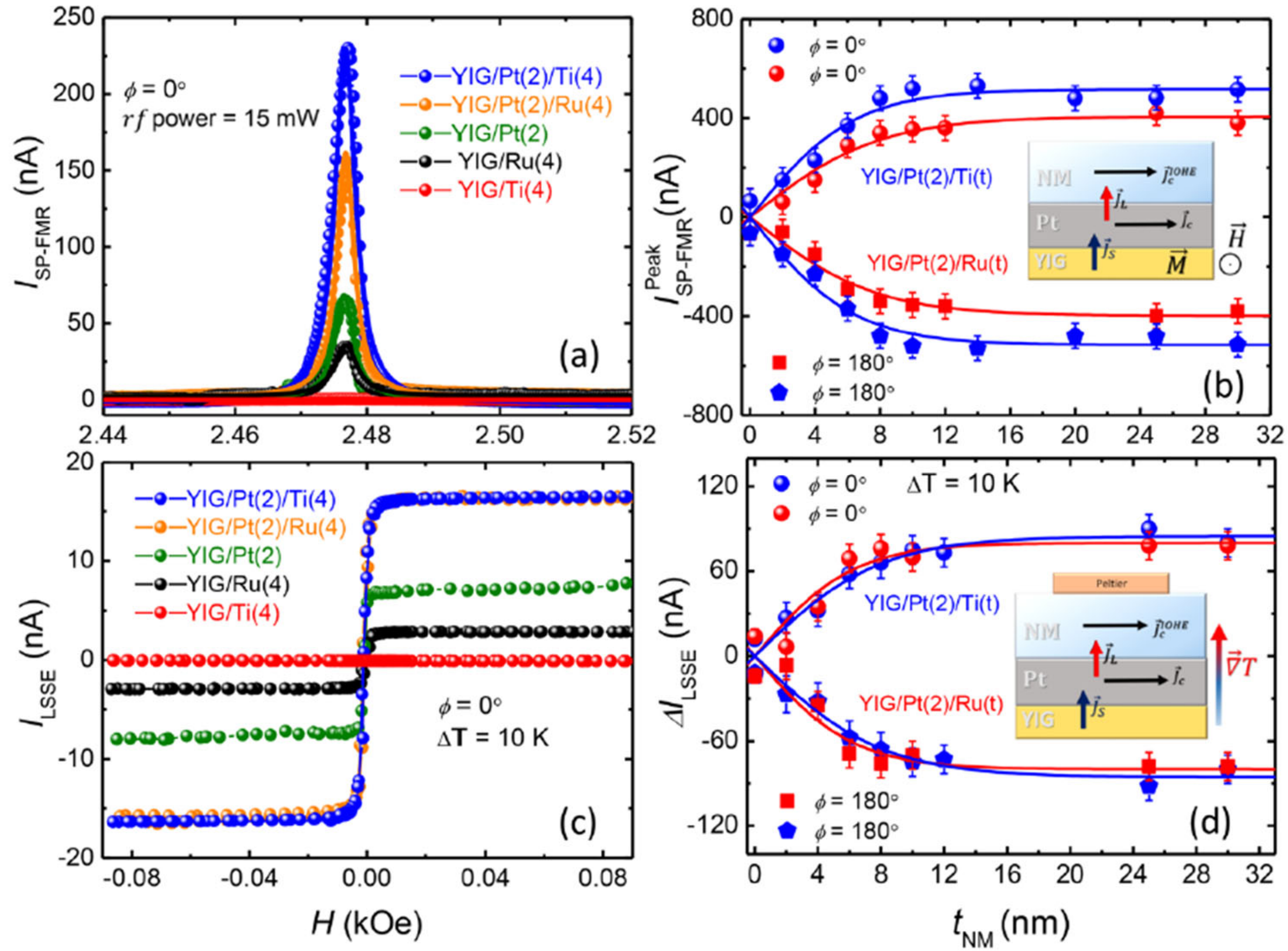

Santos et al., *ACS Appl. Nano Mater.* **8**, 4300 (2024)

Dynamic orbital-to-spin ratio in FM metals

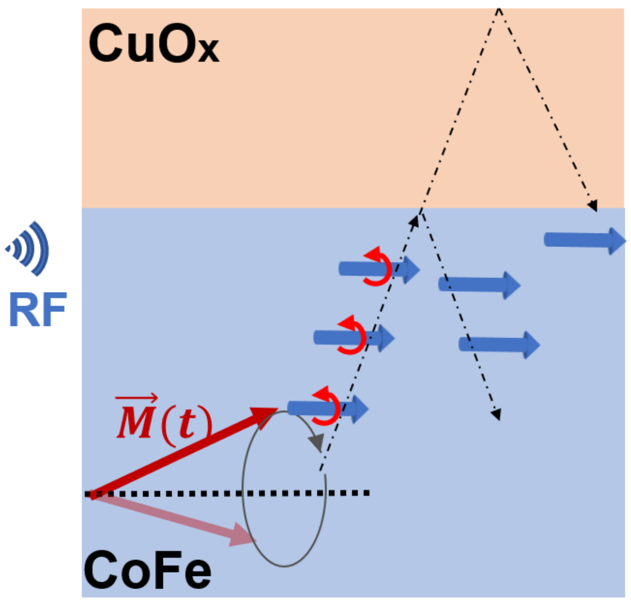

orbital pumping
$\approx 0.1 \times$
spin pumping

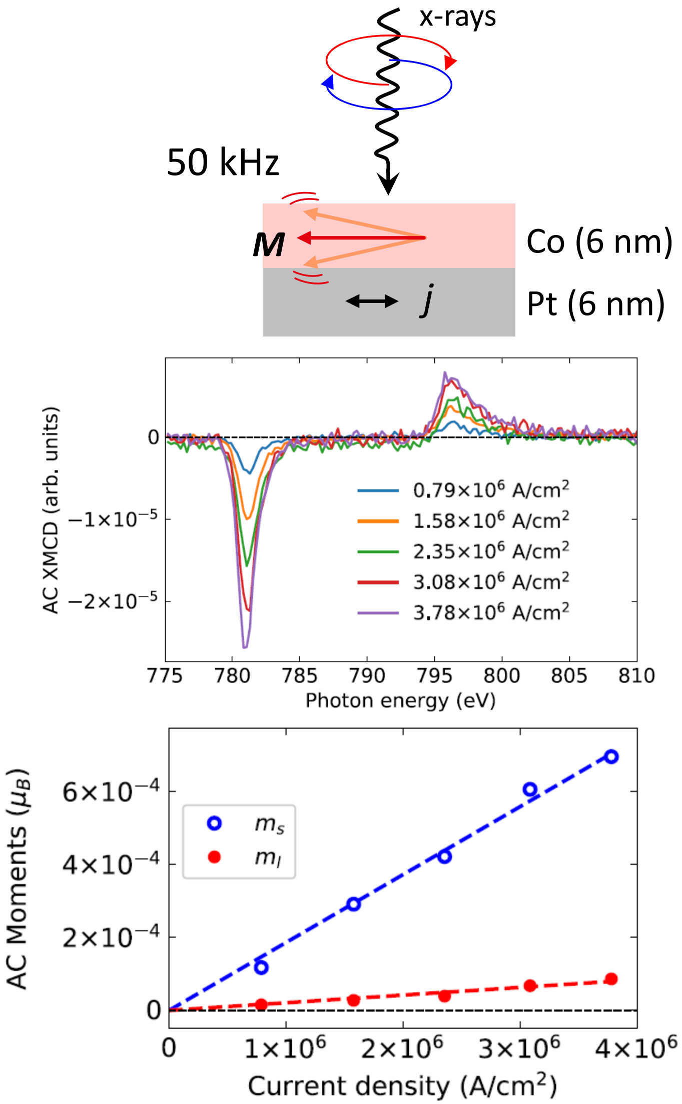

$L/2S \approx 0.12$

Stamm, PG et al., PRB **100,** 024426 (2019)

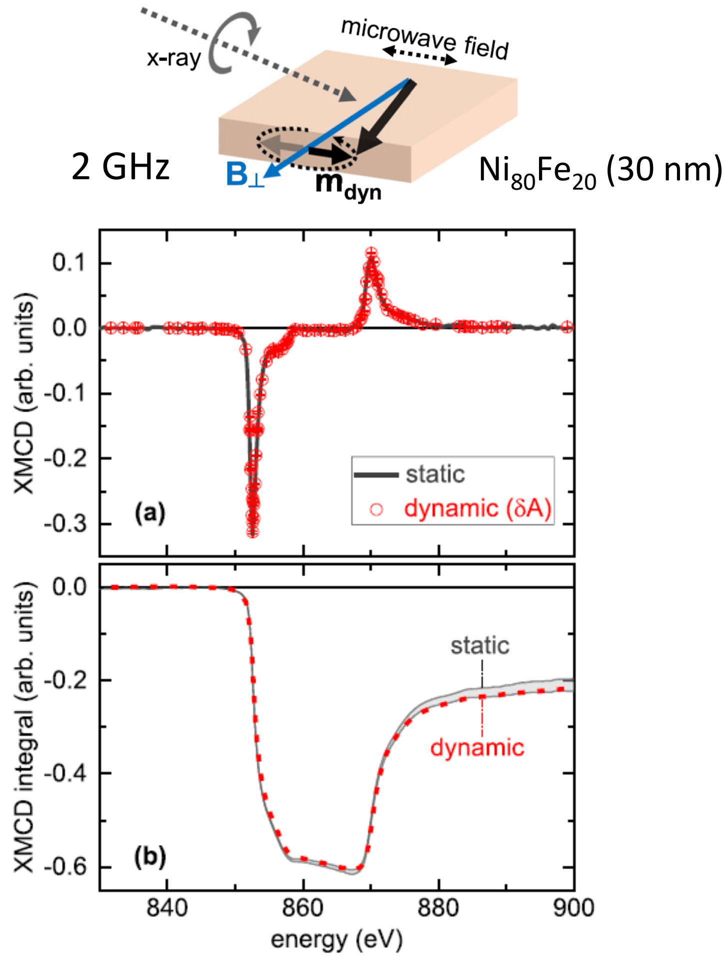

$L/2S \approx 0.11$

Emori et al., APL **124**, 122404 (2024)

Large orbital torques and small damping in $CoFe/CuO_x$

ETH zürich

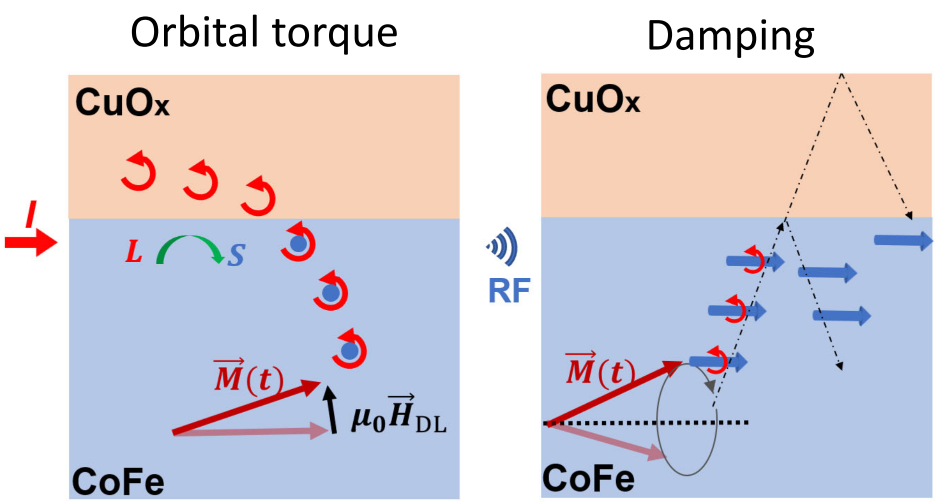

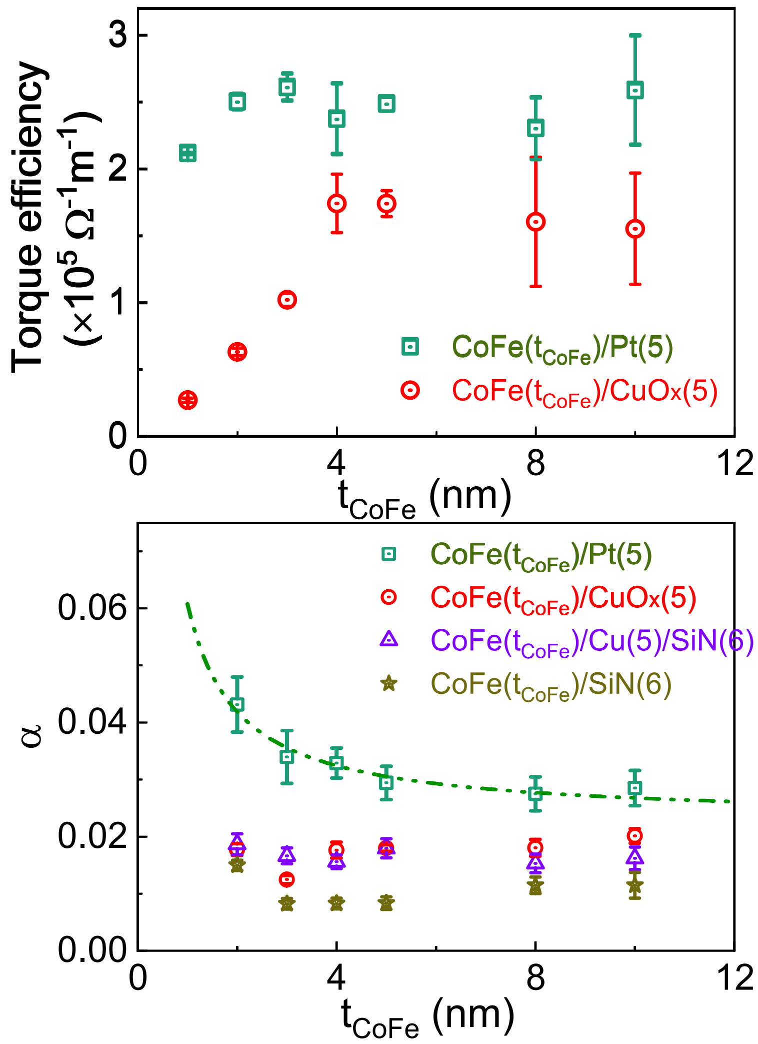

✓ Large orbital torque

✓ Small damping: $\Delta\alpha \approx 0$

S. Ding, PG et al. *Nano Lett*. **24**, 10251 (2024)

Coupling phonons to orbital momenta: the acoustic orbital Hall effect

ETH zürich

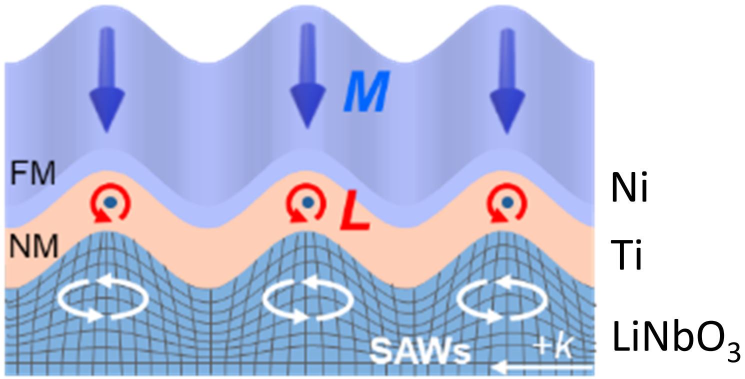

Reflection of orbital current: large V_{xx}

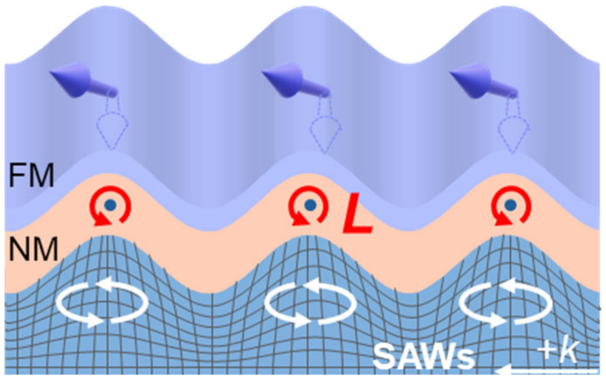

Absorption of orbital current: small V_{xx}

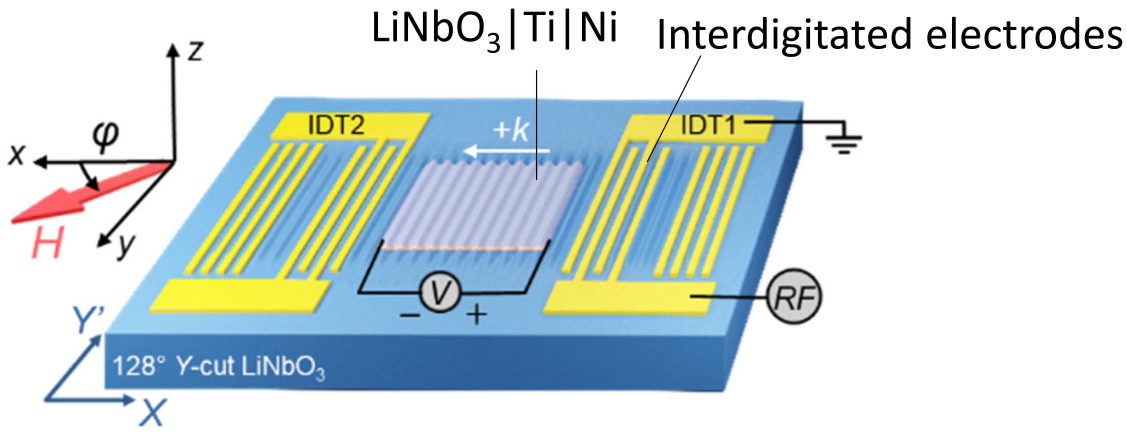

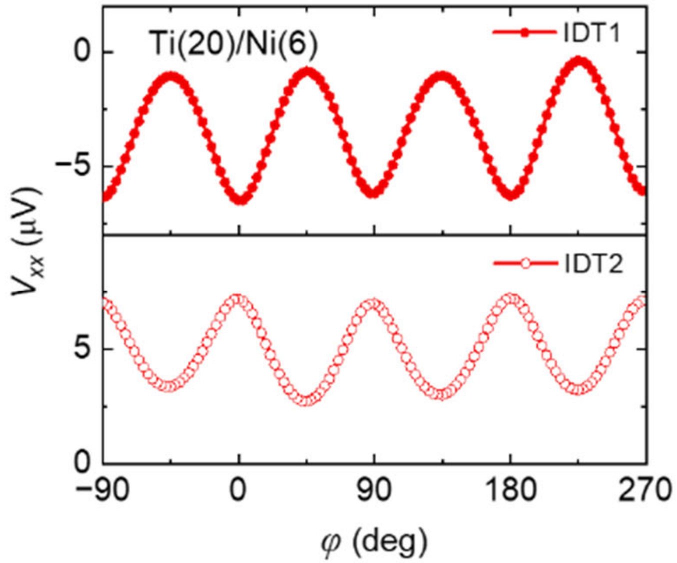

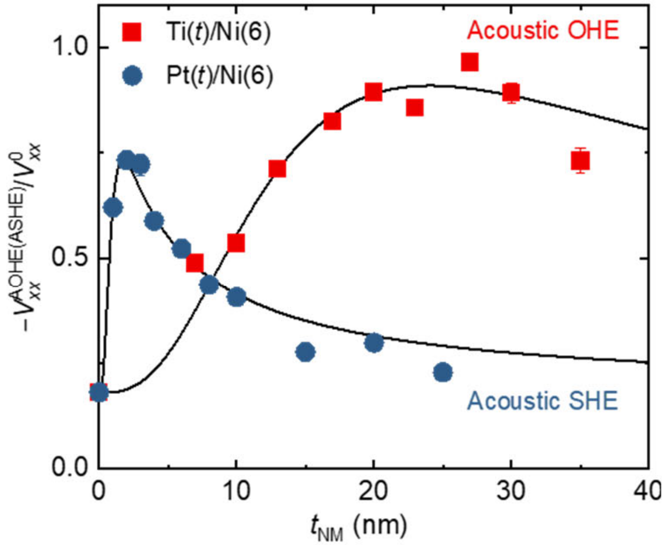

Wu, Ding, Matsumoto, PG, *arXiv*:2511.02388; Taniguchi, Haku, Lee, Ando, *Nat. Commun*. **16**, 8038 (2025); Acoustic SHE: Kawada et al., *Sci. Adv*. **7**, eabd9697 (2021)

Orbital momenta induced by optically driven phonons: the phononic Barnett effect

ETH zürich

Transient magnetization induced in a paramagnet

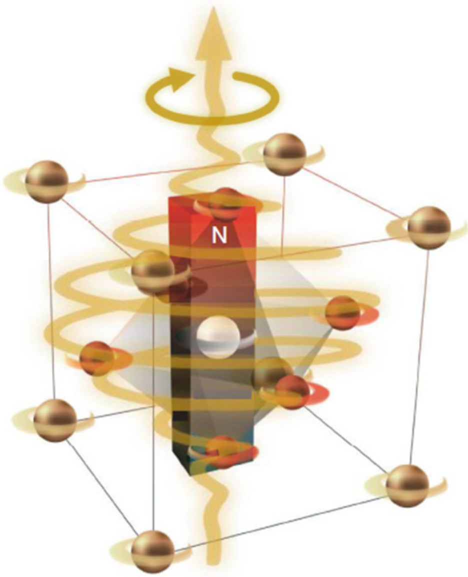

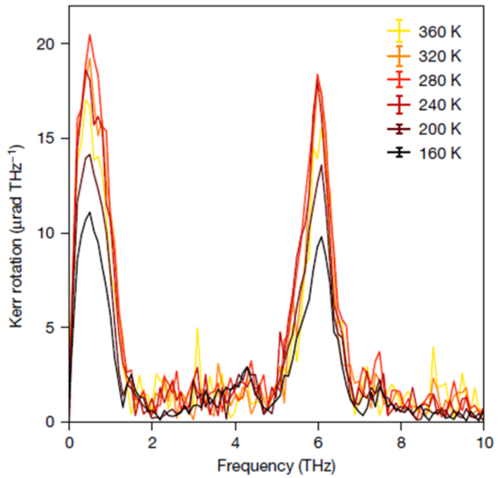

Coherent phonon excitation by a circularly-polarized THZ field in $SrTiO_3$

Kerr rotation: Transient net orbital momentum in the lattice transferred to electron system

Basini et al., Nature **628**, 534 (2024)

Switching of a nearby magnet by excitation of CP phonons

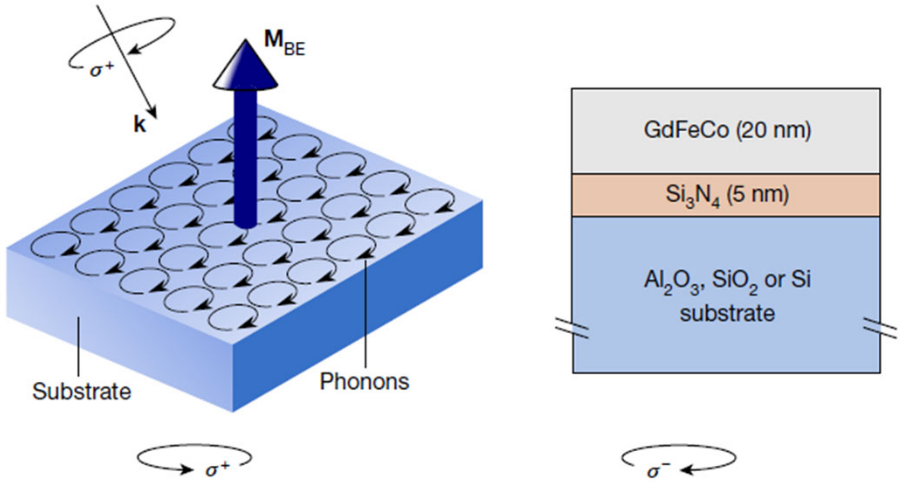

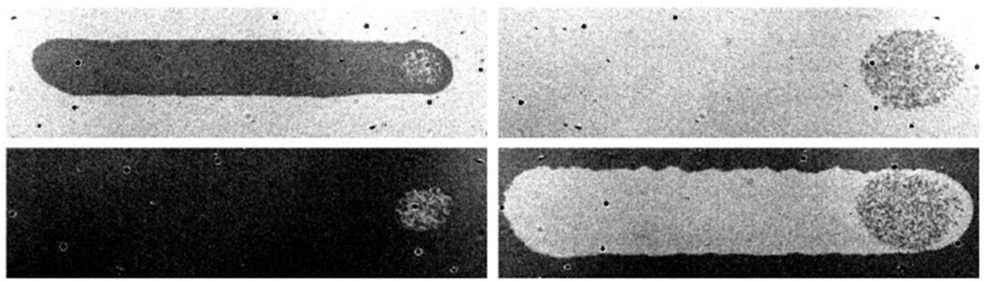

Davies et al., Nature **628**, 540 (2024)

Charge-orbital-spin conversion

- Additional degree of freedom in spintronics → orbitronics
- Improving figures of merit by material optimization
- Giant orbital torques in 3d systems
- Large orbital torque can coexist with small magnetic damping
- Tunable L/S conversion

Some open questions:

- Orbital generation mechanisms: local vs nonlocal
- Orbital transport: length- and time scales
- Coupling to quasiparticles: magnons, phonons, photons

Orbital pumping

- Orbital pumping scales with g-factor of magnetic layer
- Orbital pumping does not result in a significant increase of Gilbert dampoing due to small L/S ratio
- Electrical excitation/detection of phonon – orbital couplings